國 立 交 通 大 學
顯 示 工 程 研 究 所

碩士論文

非同步約分諧波鎖模摻鉺光纖光固子雷射之雷射動力學

Laser dynamics of asynchronous rational harmonic mode-locked Er-doped fiber soliton laser

研究生：江國豪
指導教授：賴暎杰 博士

中華民國一百零一年六月

非同步約分諧波鎖模摻鉺光纖光固子雷射之雷射動力學

研究生:江國豪　　教授:賴暎杰 博士

國立交通大學顯示工程研究所

摘要

本論文主要探討非同步約分諧波鎖模摻鉺光纖光固子雷射的雷射動力學特性，一方面透過約分諧波鎖模來達到超高重複率，也同時透過非同步鎖模來獲得良好的鎖模脈衝輸出。我們在實驗上進一步利用非同步鎖差頻的方式來補償共振腔的擾動，接著量測和探討整個雷射系統的雷射動力學。我們也利用 RF 頻譜的資訊計算出非同步約分諧波鎖模脈衝在時間上的變化和光頻的變化，利用這些結果去反推等效調變深度，並進一步驗證相位調變非同步約分諧波鎖模雷射的等效調變效應主要來源為 RF 放大器的高階分量。我們在探討雷射動力學的時候也發現了一個新的同步諧波鎖模雷射操作模態，可以產生重複率高達 40GHz 的穩定鎖模脈衝雷射並在 RF 頻譜觀察到邊頻項，透過設計一連串的實驗我們也探討了這個有趣新穎的新操作模態。

Laser dynamics of asynchronous rational harmonic mode-locked Er-doped fiber soliton laser

Student: Guo-Hao Jiang **Advisor: Dr. Yinchieh Lai**

Institude of Display, National Chiao-Tung University

Abstract

The thesis is focused on the laser dynamics studies of asynchronous rational harmonic mode-locked Er-doped fiber soliton lasers. The rational harmonic mode-locking can provide higher repetition rates and the asynchronous mode-locking can help achieve good mode-locking performance. We stabilize the laser cavity length by locking the deviation frequency of asynchronous mode-locking to help measure the laser dynamics of the laser system. Base on the information of the RF spectra, we estimate the timing and center frequency variation of the asynchronous rational harmonic mode-locked pulse trains. We verify that the effective modulation strength is mainly from the higher order signals of the RF amplifier in asynchronous rational harmonic mode-locked lasers with only phase modulation. We also experimentally find a new

operation state of synchronous harmonic mode-locking. Stable 40 GHz mode-locking operation can be achieved with RF spectral sidebands quite similar to the asynchronous mode-locking. A series of experiments have been performed to investigate the characteristics of this interesting new operation state.

誌謝

在實驗室短短的兩年裡因為實驗上的需要學習到好多知識和解決問題的能力，雖然實驗中遇到許多不可預期的困難，但最後都一一解決了，現在要和實驗室的大家說再見並感謝大家一路的幫助。

首先要感謝的是我的指導教授賴暎杰，老師在我有問題的時候總是很有耐性的跟我解釋，這些問題並不侷限在專業的知識上，在我徬徨無助的人生路上，老師也能給予我適當的建議以及不同的想法，帶著老師所指導的一切離開學校我覺得心滿意足，在未來的日子裡一定不負老師的教誨一步一步實踐我的夢想。

感謝實驗室實力堅強的學長姊們：鞠曉山學長、項維巍學長、徐桂珠學姊、許萓蓁學姊、吳尚穎學長、王聖閔學長不僅教會我使用儀器的方法還有解釋實驗數據的方式，你們許多寶貴的意見學弟我都有聽到並吸收，這些珍貴的經驗傳授讓我能更快達到實驗的目標。

也要感謝實驗室的夥伴們，楊良愉、林仕斌、黃耀德、顧戎，實驗室有你們的陪伴樂趣增加不少，在我因為實驗不順利心情不好時你們陪我聊天陪我玩 LOL(英雄聯盟)舒緩我的壓力，讓我更有動力面對接下來的問題。

最後要感謝我的家人還有我的女朋友洪詩婷，在我努力認真求學的階段裡一直陪伴著我。

Contents

Chapter 3: Experimental setup and results

Chapter 4: Conclusions

List of Figures

Chapter 1

Introduction

1.1 Overview

A fiber laser is a laser in which the gain medium is an optical fiber doped with rare-earth elements such as erbium (1550nm) and ytterbium (1060nm). The 1550nm wavelength region has the lowest fiber propagation loss and has been widely utilized as the fiber communication spectral window. Because of this, the erbium-doped fiber laser is most suitable for optical communication purposes and has also been popularly applied in the measurement equipment. In contrast, the ytterbium-doped fiber laser is most suitable for industrial applications due to the achievable high output power and conversion efficiency.

According to the gain medium type, we can classify lasers into categories of gas, liquid, and solid state. Gas state laser like CO_2 laser can be applied for many applications required high power. Semiconductor laser is one of the most common types of solid state lasers. It is suitable to be integrated with electrical devices due to their electrical pumping characteristics. However, for generating ultrashort optical pulses, the mode-locked fiber laser would be more suitable than many other lasers

due to the large gain bandwidth of rare-earth-doped fibers, which is essential for producing ultrashort pulses. Ultrashort pulse can help avoid organism tissue damage resulted from the heat heap. Because of this, ultrashort pulse laser is also popularly applied in the area of biophotonics.

Typically there are two ways to achieve mode-locking of the lasers. One is the passive mode-locking and the other is the active mode-locking. The passive mode-locking can generate shorter pulses than active mode-locking while the active mode-locking can generate higher repetition rates than the passive mode-locking. One can also employ hybrid mode-locking which contains these two mode-locking mechanisms to generate ultrashort pulse trains in the high repetition rates.

However, in practice there are still many other problems needed to be solved. One of the most important issues is the environmental perturbation resulted from the effects of expanding when hot and shrinking when cold. This effect apparently influences the stability of active mode-locked fiber lasers due to the cavity length variation caused by environmental temperature perturbation, because in general, active mode-locking is possible only when the modulation frequency and the harmonic mode frequency in the cavity can synchronize. Since it is not

practical to set up systems in the experimental environments without perturbations, it is thus crucial to know how to employ a feedback control loop to compensate the cavity length variation.

In the past literature, many methods have been used to help maintain the pulse train of high repetition rates in mode-locked fiber lasers. By installing an optical etalon in the laser cavity, a regenerative mode-locked fiber laser can achieve mode-hop-free operation [1.1]. Another economic way is to employ asynchronous mode-locking scheme. The feedback stabilization control can be achieved by detecting the deviation frequency between the modulation frequency of phase modulation and the harmonic frequency of the cavity. In this way the error signal can be utilized to control the optical delay line to correct the cavity length for laser stabilization..

Recently, asynchronous mode-locked Er-doped fiber soliton laser has been investigated extensively. Direct generating of 10GHz 816 fs pulse train from an erbium-fiber soliton mode-locked fiber laser with asynchronous phase modulation has been demonstrated [1.2]. Applying asynchronous mechanism to stabilize high repetition rate fiber lasers for long time operation has also been successfully demonstrated [1.3]. Even

though harmonic mode-locking can generate high repetition rate pulse trains, it is still limited by the available modulation frequency. It will be nice to have some other methods to increase the repetition rate. One of these methods is to employ the rational harmonic mode-locked mechanism by detuning the modulation frequency with a rational order of the fundamental frequency of the cavity [1.4]. This kind of high repetition rate mode-locked fiber lasers that can output ultrashort pulse trains is suitable for high speed optical communication and ultrafast optical signal processing [1.5].

1.2 Motivation

Asynchronous mode-locked fiber soliton lasers have been attractive due to the low cost stabilization method and the high supermode suppression ratio (SMSR). It is natural to expect that by combining the asynchronous mode-locking mechanism and the rational harmonica mode-locking mechanism, one may be able to generate high repetition rate pulse trains without being limited by the synthesizer frequency and without suffering from the environmental perturbations. However, the laser dynamics of asynchronous rational harmonic mode-locked Er-doped

fiber soliton lasers have not been well studied. It will be important to understand more about their laser dynamics before one can actually develop their applications.

1.3 Organization of this thesis

This thesis consists of four chapters. Chapter 1 is an overview of the fiber laser development and the motivation for carrying out this research. Chapter 2 describes the methods of active mode-lockingand discusses the issues of rational harmonic mode-locking, asynchronous mode-locking, and long-term stabilization of mode-locked fiber lasers. Chapter 3 presents the experimental setup and analyzes the results of experiments. Finally, Chapter 4 gives a summary about our achievements and possible future work.

Reference

[1.1] M. Yoshida, K. Kasai and M. Nakazawa, “Mode-hop-free optical frequency tunable 40 GHz mode-locked fiber laser,” IEEE J. Quantum Electron. **8,** 704 (2007).

[1.2] W. W. Hsiang, C. Y. Lin, M. F. Then and Y. Lai, “Direct generation of a 10 GHz 816 fs pulse train from an erbium-fiber soliton laser with asynchronous phase modulation,” Opt. Lett. **18**, 2493 (2005).

[1.3] W. W. Hsiang, C. Y. Lin, N. Sooi and Y. Lai, “Long-term stabilization of a 10 GHz 0.8 ps asynchronously mode-locked Er-fiber soliton laser by deviation-frequency locking,” Opt. Express **5**, 1822 (2006).

[1.4] C. Wu and N. K. Dutta, “High-repetition-rate optical pulse generation using high-repetition-rate optical pulse generation using,” IEEE J. Quantum Electron. **2**, 145 (2000).

[1.5] J. P. Wang, B. S. Robinson, S. A. Hamilton, and E. P. Ippen, “Demonstration of 40-Gb/s packet routing using all-optical header processing,” IEEE Photon. Technol. Lett. 21, 2275 (2006).

Chapter 2

Theories of mode-locked fiber lasers

2.1 Active mode-locking

The active mode-locking mechanism is based on the active modulation which induces the loss or phase modulation in the laser cavity. The utilized active modulators may be either the acousto-optic or the electro-optic modulators. If the modulation frequency is synchronized with the resonator round trip time, the optical pulse trains in the cavity will continue to grow and finally achieve stable mode-locking (Fig. 2.1).

In general, active mode-locked fiber lasers can use two different methods for optical modulation. One is the amplitude modulation (AM) mode-locking, and the other is the phase modulation (PM) mode-locking. Detailed introduction for the two general methods of modulation will be given in the following section.

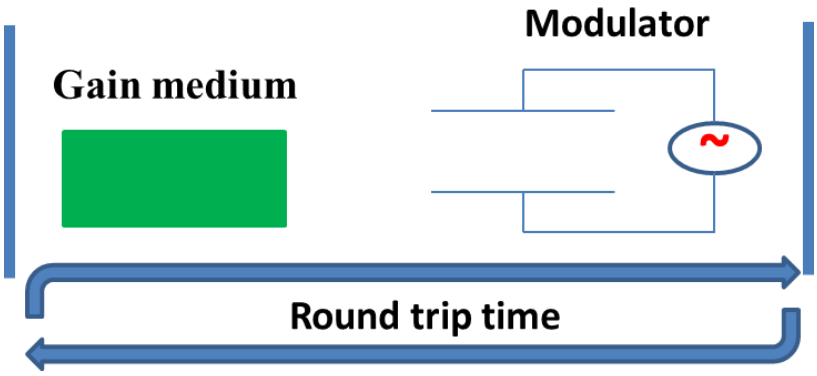

Fig. 2.1 Schematic of an active mode-locked laser

2.1.1 Amplitude modulation mode-locking

Amplitude modulation mode-locking is a way in which the optical amplitude is modulated directly to produce a short pulse train. This mechanism can be analyzed both in the frequency domain and the time domain [2.1].

In frequency domain, as the net gain of the system is greater than zero, longitudinal modes will start to lase. The longitudinal modes are separated equally in the frequency domain and the frequency interval is $\Delta\Omega = \frac{2\pi}{T_R}$, where T_R is the round trip time. Denoting the center frequency to be ω_0, the sidebands which center on ω_0 will grow together as explained below if the lasers carry out mode-locking by the method of amplitude modulation.

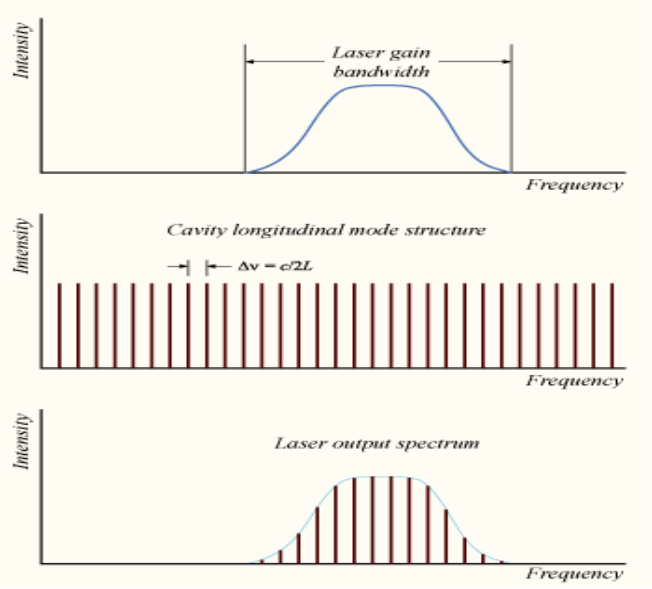

Fig. 2.2 Actively mode-locked modes in the frequency domain

Assuming the optical signal in the resonator is $\mathrm{E(t)} = E_0 \cos(\omega_0 t)$, then the amplitude modulated optical signal can be expressed as below:

$$\mathrm{E(t)} = (1 + \mathrm{M}\cos(\Omega_m \mathrm{t}))E_0 \cos(\omega_0 t)$$

$$= \mathrm{E_0}\cos(\omega_0 \mathrm{t}) + \mathrm{E_0}\frac{\mathrm{M}}{2}\cos(\omega_0 + \Omega_\mathrm{m})\,\mathrm{t} + \mathrm{E_0}\frac{\mathrm{M}}{2}\cos(\omega_0 - \Omega_m)\mathrm{t} \quad (2\text{-}1)$$

Here we have denoted the modulation depth and modulation frequency to be M and Ω_m respectively. According to above results, the center frequency ω_0 produces two inphase sidebands $(\omega_0 \pm \Omega_\mathrm{m})$ after the modulation. If one applies the amplitude modulation again other two inphase sidebands $(\omega_0 \pm 2\Omega_\mathrm{m})$ can be produced. After repeating the process of modulation, the longitudinal modes in the gain profile will be all phase-locked and the mode-locking can be achieved finally.

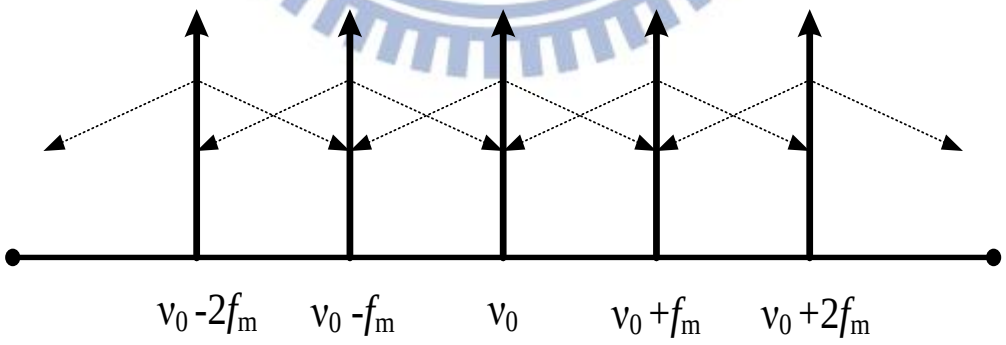

Fig. 2.3 Diagram of the amplitude modulation mode-locking in the frequency domain.

In the time domain analysis, the modulator produces a periodic loss in the cavity. Pulse trains builds up when the gain is greater than the

loss. If the optical signal passes through the maximum transmission point every roundtrip, then the optical signal will be amplified again and again until it reaches the steady state. The pulsewidth become shorter after passing through the amplitude modulator repeatedly. The pulse shortening strength caused by modulation balances the pulse broadening strength caused by the dispersion/filtering effects of the cavity in the steady state. The modulation time period must be either equal to the roundtrip time of the laser cavity or equal to the integer fractional of the roundtrip time for the cases of harmonic mode-locking.

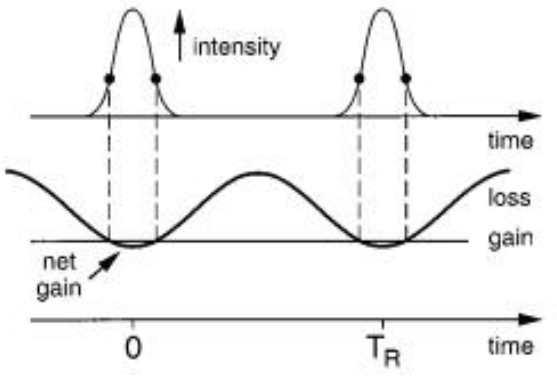

Fig. 2.4 Actively mode-locked pulses in the time domain and the time dependence of the net gain.

The master equation of amplitude modulation mode-locked lasers can be written as:

$$T_R \frac{\partial u(T,t)}{\partial T} = (g - l)u(T,t) + \frac{g}{\Omega_g}\frac{\partial^2}{\partial t^2}u(T,t) - \frac{1}{2}M\Omega_M t^2 u(T,t) \qquad (2\text{-}2)$$

where g is the gain per pass, l is the loss, Ω_g is the gain bandwidth and M is the modulation index.

2.1.2 Phase modulation mode-locking

Phase modulation mode-locking is a way in which the optical signal is phase modulated directly to produce short pulse trains. This mechanism again can be analyzed both in the frequency domain and the time domain.

In the frequency domain, we assume the center frequency is ω_0 as before. When the longitudinal mode is modulated by passing through the phase modulator, the optical signal can be written as below:

$$E(t) = E_0 \cos(\omega_0 t + M\cos\Omega_M) \quad (2\text{-}3)$$

$$= E_0 \sum_{-\infty}^{\infty} J_n(M)\cos(\omega_0 t + n\Omega_M t) \quad (2\text{-}4)$$

where M is the modulation index, Ω_M is the modulation frequency and J_n is the n-th order Bessel function.

It can be seen that the optical signal consist of unlimited sidebands when (2-3) is expanded into (2-4). The periodic pulse trains are formed when the phases of different modes are mode-locked. The pulse trains diagram is shown in Fig. 2.5

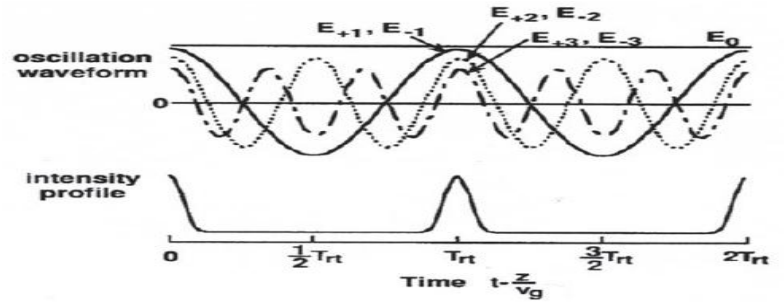

Fig. 2.5 Formulation of pulse trains in the time domain.

In the time domain, the phase of the optical pulse will be changed by the phase modulator. In the beginning, we can set the constant phase without modulation effect is φ_0. Then the optical phase changed by the phase modulator can be expressed by a Taylor series and the result is written as below:

$$\varphi(t) = \varphi_0 + \frac{d\varphi}{dt}t + \frac{d^2\varphi}{dt^2}t^2 + \dots \quad (2\text{-}5)$$

where $\frac{d\varphi}{dt}$ means the immediate frequency. When $\frac{d\varphi}{dt} \neq 0$, the modulation will cause the frequency shift of the optical pulse. Central frequency will continue to be shifted when passing through the phase modulator per round trip, until the optical pulse is shifted out of the gain bandwidth and disappears. As a result, only the synchronized pulses can survive in the laser cavity and then reach the steady state. However, $\frac{d\varphi}{dt} = 0$ has two solutions (positive 2nd order derivative and negative 2nd order derivative). There will be only one stable solution depending on the

sign of $\frac{d^2\varphi}{dt^2}$ and the sign of the cavity dispersion.

2.2 Rational Harmonic mode-locked fiber laser

The high repetition rate mode-locked fiber laser may be useful for high bit rate optical communication systems. The active mode-locking of Er-doped fiber lasers is an attractive way for achieving mode-locking because it can offer transform-limited, sub-picosecond pulse trains with a repetition rate of 10 GHz or higher [2.2] [2.3]. However, the repetition rate of fiber laser is limited by the bandwidths of the electro-optic modulator, synthesizer and RF power amplifier. Rational harmonic mode-locked (RHML) technique can overcome this problem and thus it has attracted a great deal of interest. The method is to detune the modulation frequency away from the longitudinal mode of harmonic mode-locking (HML) to generate high repetition rate pulse trains [2.4].

In this mode-locked mechanism, the final repetition rate can be

$$(\mathrm{np}+1)f_c \tag{2-6}$$

when the modulation frequency is set at

$$(\mathrm{n}+\tfrac{1}{p})f_c \tag{2-7}$$

Note that f_c is the fundamental frequency of the cavity

$$f_c = \frac{c}{n_{eff} * L} \quad (2\text{-}8)$$

Here n and p are integrals, c is the optical speed in the vacuum and n_{eff} is the effective index of the cavity and L is the cavity length.

By using the RHML laser configuration, Nakazawa and Yoshida have achieved high repetition rate rational harmonic mode-locked fiber laser up to 80-200GHz [2.5]. L. R. Chen has demonstrated wavelength-tunable, 30-GHz pulse train generation from a rational harmonic mode-locked fiber optical parametric oscillator (FOPO) by using a 10-GHz driving source [2.6].

If the fiber laser is applied to practical systems, the stability of the optical pulse trains from a fiber laser needs to be improved. The instability may originally come from three main causes:

1) Polarization fluctuations in the long fiber cavity due to fiber vibrations,
2) Cavity length drifts due to the temperature fluctuations.
3) Supermode noises which frequencies could be any integral multiples of the cavity fundamental frequency.

Several approaches have been developed to overcome these problems. Nakazawa and Yoshida constructed the fiber lasers with an

all-polarization-maintaining ring cavity [2.3] [2.7]. The issues about how to stabilize the fiber cavity length from not being suffered from the fluctuations in the temperature will be given in Chapter 2.4.

However, the most important problem in the rational harmonic mode-locking is the pulse amplitude variation. Considering a simple example when $f_m = (1 + \frac{1}{3})f_c$, the diagram of light modulation in the ring cavity is shown in Fig. 2.6.

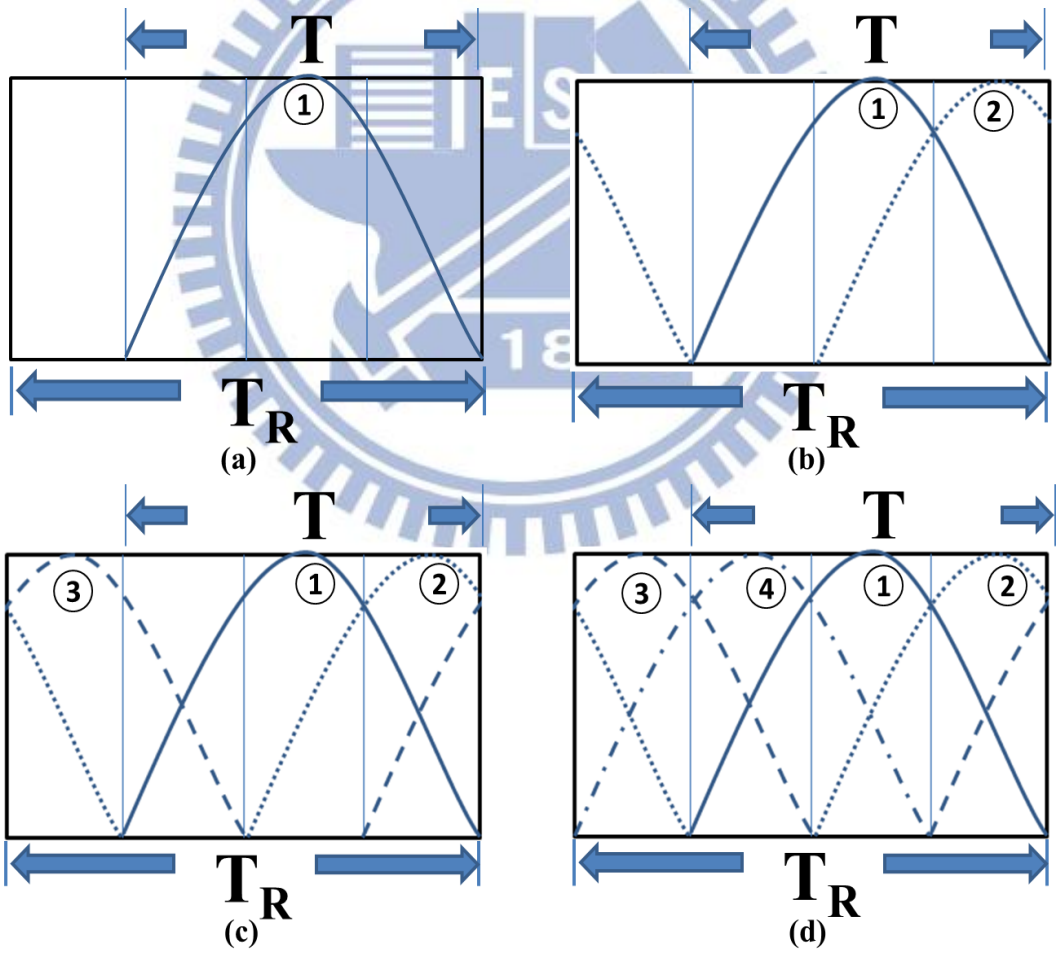

Fig. 2.6. Sketch of light modulation in the cavity after T, 2T, 3T, 4T respectively

When light is modulated in the cavity after T, 2T, 3T, 4T respectively,

this process will continue to go through repeatedly. The lights in the cavity are amplified and eventually form the pulse trains in the particular position of time domain as shown in the Fig. 2.7 (a).

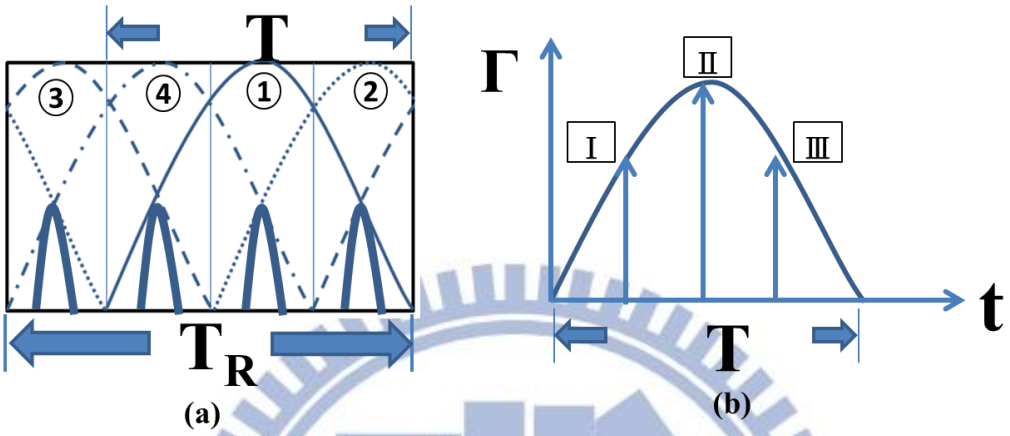

Fig. 2.7 (a) Pulse train in the particular position of time domain. (b) Pulse in the modulation transmission curve at immediate time

In Fig. 2.7 (b), the pulse forms and gets modulated at I, II, II sequentially in three time periods. So for the $P = 3$, the pulse can be generated in the three points of the modulation curve, but their transmission ratios are different in different time periods. That is the reason why the amplitude variation usually occurs in the rational harmonic mode-locked fiber lasers.

To solve this problem, several researches have been reported for amplitude equalization. By properly adjusting the bias level of the

modulator one can equalize the amplitude [2.8]. N.K. Dutta has applied this equalized technique to demonstrate a rational harmonic mode-locked fiber laser with amplitude-equalized output operating at 80 Gbits/s [2.9]. Another main technique for equalizing the pulse amplitude is by using the SOA [2.10].

Rational harmonic mode-locking can be carried out by an amplitude modulator or a phase modulator [2.11]. X. Bao gave a conclusion that rational harmonic mode-locking can be achieved by using the phase modulation and better performance than the counterpart with amplitude modulation can be expected [2.12].

2.3 Asynchronously mode-locked fiber laser

In active harmonic mode-locked lasers, the modulation frequency must exactly be equal to the cavity harmonic frequency, since otherwise the pulse trains cannot build up in the cavity. This is because the optical pulses will be shifted by a frequency if not synchronized. In the presence of finite bandwidth filter and gain, the pulse train cannot achieve stable mode-locking. However, in the asynchronous mode-locking mechanism [2.13], the modulation frequency is detuned from the cavity harmonic frequency by several kHz to tens kHz and stable mode-locking still can be achieved [2.14]. For the explanation of asynchronously mode-locking mechanism, it is not difficult to know from the simple diagram shown in the Fig. 2.8

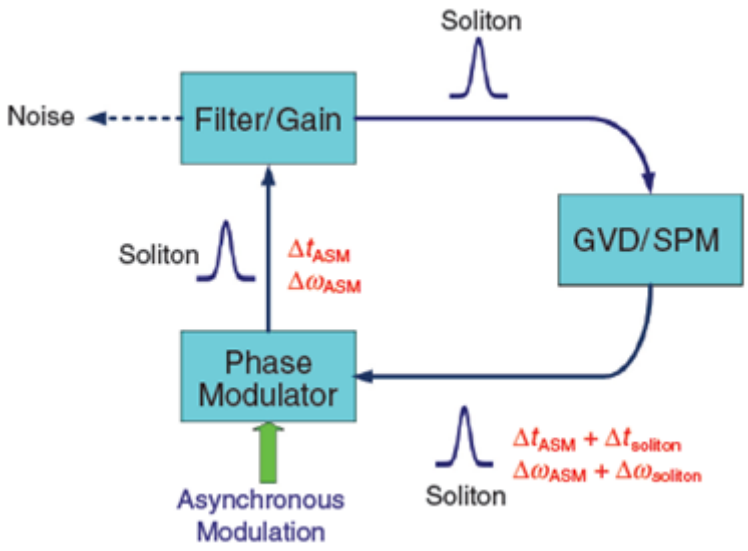

Fig. 2.8 Laser cavity with the gain, filter, group velocity dispersion (GVD), self phase

modulation (SPM) and the phase modulation driven asynchronously.

The fiber laser of Fig. 2.8 is consisted of the optical bandpass filter, group velocity dispersion (GVD), self phase modulation (SPM), gain medium and the phase modulator. Under this laser configuration, the pulse does not disappear in the cavity. On the contrary, stable pulse trains can be realized and compressed to sub-picosecond pulse-width with the 10GHz repetition rate [2.15]. The noise clean up mechanism is similar to the effects of sliding-frequency guiding filters in soliton communication systems [2.16]. The soliton effects induced by the fiber nonlinearity in the asynchronous mode-locked fiber laser can help the mode-locked pulses to survive the asynchronous phase modulation. As a result, the solitons can exist steadily in the cavity, as is shown in Fig. 2.9.

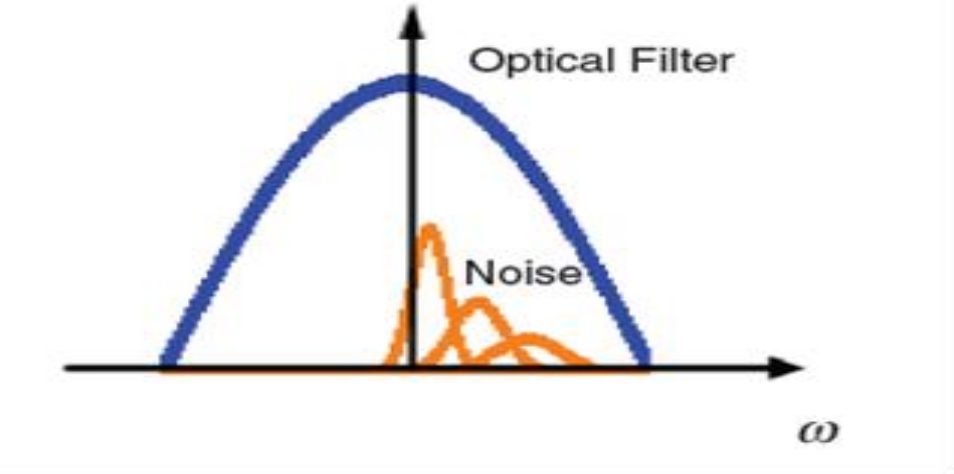

Fig.2.9 The noise-cleanup effect in the asynchronous mode-locked soliton laser.

The central frequency of the solitons varies in the fiber cavity during

propagation, but the central frequency of the linear noises keep fixed and will be filtered out by the optical filter. So the asynchronous mode-locking mechanism can provide high SMSR performance without requiring additional intracavity optical devices [2.17].

Applying asynchronous mode-locking in fiber lasers to generate ultra-short pulses provides other advantages. One is to utilize the deviation frequency for feedback use. The other is to take advantages of the laser dynamics of asynchronous mode-locked fiber lasers for special applications [2.18]. These two aspects will be discussed in Chapter 2.4 and Chapter 3.

2.4 Long-Term Stabilization of Mode-Locked fiber laser

The generation of ultrashort optical pulses in the GHz level is very important for high bit rate optical communication and optical metrology [2.19]. The most common way to produce high speed optical pulse trains is through active mode-locking. In the literature, many techniques have been carried out. These techniques include synchronous mode-locking, asynchronous mode-locking, rational harmonic mode-locking and regenerative mode-locking [2.20].

When the laser speed is improved to the GHz level, applications in practical systems still require enhancing the stability of optical pulse trains. There are many researches to reduce the noises for achieving long-term stabilization of the mode-locked fiber laser. They are as given in the below:

A) PZT

The main cause for laser instability is the cavity length drift due to the temperature fluctuations. This perturbation causes the repetition rate to shift and then the mode-locking cannot be maintained. The supermodes may also oscillate simultaneously and compete with each other. Thus the

fluctuations of pulse amplitude are generated, which appear as noises in the RF spectrum.

As said above, controlling the cavity length is a direct way to enhance the stability. It can use the error signal from the mixing of the modulation frequency signal and the pulse repetition rate signal to control the voltage of PZT. The PZT is lengthened or shorted by the applied voltage. The length of fiber winded around the PZT is thus also changed by the error signal. Finally, the cavity length fluctuations caused by temperature perturbations can be compensated and a fixed cavity length can be kept [2.21].

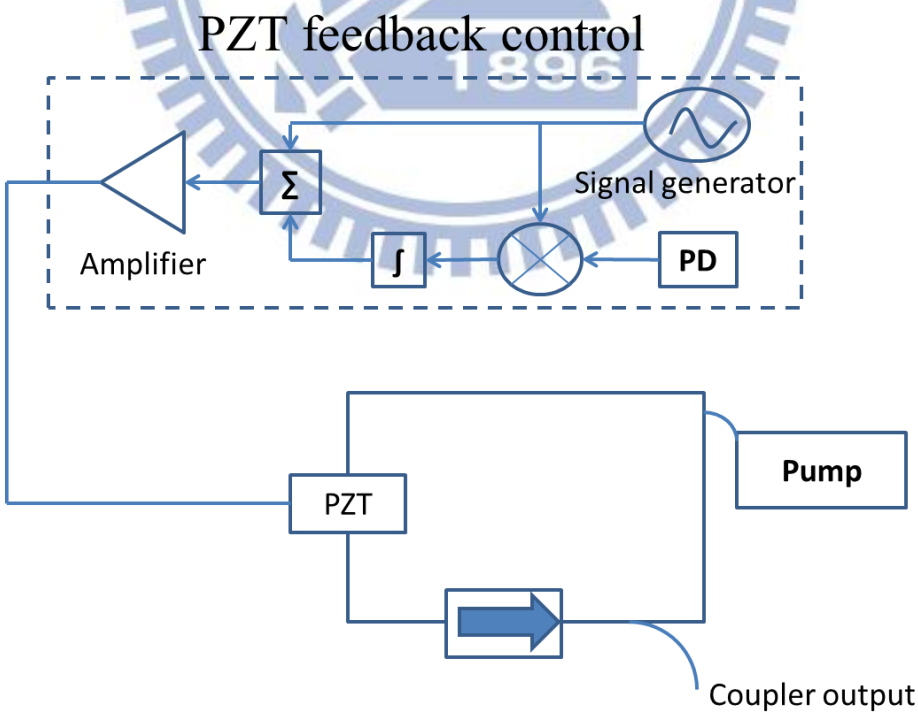

Fig. 2.10 Schematic setup of PZT feedback control

B) Regenerative mode-locking [2.3]

As shown in Fig. 2.11, the 40GHz clock extraction circuit is used to extract the 40 GHz clock from the laser output. The clock is then amplified and applied to the phase modulator. Finally, mode-locking is carried out. The laser operation continued stably for a long time because the modulation frequency (i.e. clock signal) always follows the changes in the cavity length. This means the modulation frequency and the cavity harmonic frequency always keep synchronous.

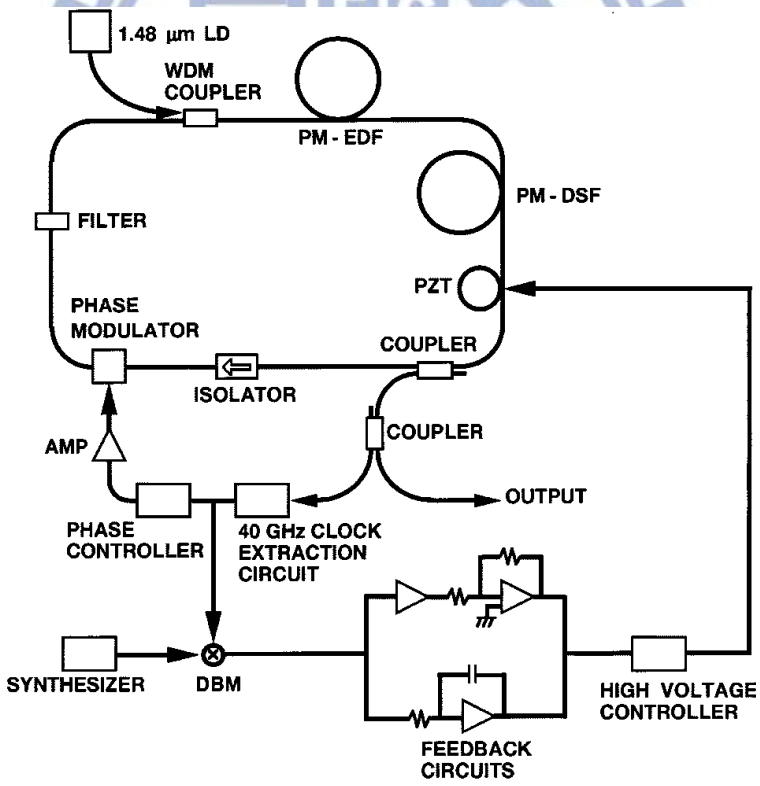

Fig. 2.11 Diagram of regenerative mode-locked fiber laser

Recently, the mode-locked fiber laser stabilization techniques are improved to a more advanced level. Base on the regenerative

mode-locked technique, Nakazawa and Yoshida have successfully demonstrated the mode-hop-free optical frequency tunable mode-locked fiber laser [2.22].The wavelength reference of C_2H_2 is employed to absolutely stabilize the optical frequency of the mode-locked fiber laser [2.23]. It is also possible to independently stabilize the repetition rate and the optical frequency [2.24].

Base on controlling the cavity length to lock the deviation frequency at a suitable value, there is a stabilization technique by taking advantages of the unique characteristics of asynchronous mode-locking [2.25]. It provides an advantage that the feedback module does not require high frequency electronics and in principle the cost can be much less.

Reference

[2.1] H. A. Haus, “Mode-locking of lasers,” IEEE J. Quantum Electron. **6**, 117 (2000).

[2.2] B. Bakhshi, P. A. Andrekson, “40 GHz actively modelocked polarization maintaining erbium fiber ring laser”, Electronics Lett. **5**, 411 (2000).

[2.3] E. Yoshida and M. Nakazawa, “A 40-GHz 850-fs regeneratively FM mode-locked polarization-maintaining Erbium fiber ring laser”, IEEE Photon. Technol. Lett. **12**, 1613 (2000).

[2.4] C. Wu and N. K. Dutta, “High-repetition-rate optical pulse generation using a rational harmonic mode-locked fiber laser,” IEEE J. Quantum Electron. **2**, 145 (2000).

[2.5] E. Yoshida and M. Nakazawa, “80~200 GHz erbium doped fiber laser using a rational harmonic mode-locking technique,” Electron. Lett. **15**, 1370 (1996).

[2.6] J. Li, T. Huang, and L. R. Chen, “Rational harmonic mode-locking of a fiber optical parametric oscillator at 30 GHz,” IEEE J. Photon. **3**, 468 (2011).

[2.7] E. Yoshida and M. Nakazawa, “Ultrastable harmonically and

regeneratively mode-locked polarization-maintaining erbium fiber ring laser," IEEE Electronics Lett. **19**, 1603 (1994).

[2.8] X. Feng, Y. Liu, S. Yuan, G. Kai, W. Zhang, and X. Dong, "Pulse-amplitude equalization in a rational harmonic mode-locked fiber laser using nonlinear modulation," IEEE Photon. Technol. Lett. **8**, 1813 (2004).

[2.9] G. Zhu and N. K. Dutta, "Eighth-order rational harmonic mode-locked fiber laser with amplitude-equalized output operating at 80 Gbits/s," Opt. Lett. 17, 2212 (2005).

[2.10] X. Feng, Y. Liu, S. Yuan, G. Kai, W. Zhang, and X. Dong, "Pulse-amplitude equalization in a rational harmonic mode-locked fiber laser using nonlinear modulation," IEEE Photon. Technol. Lett. **8**, 1813 (2004).

[2.11] S. Yang and X. Bao, "Rational harmonic mode-locking in a phase modulated fiber laser," IEEE Photon. Technol. Lett. **12**, 1332 (2006).

[2.12] S. Yang, J. Cameron, and X. Bao, "Stabilized Phase-Modulated Rational Harmonic Mode-Locking Soliton Fiber Laser," IEEE Photon. Technol. Lett. **19**, 393 (2007).

[2.13] C. R. Doerr, H. A. Haus, and E. P. Ippen, “Asychronous soliton mode locking”, Opt. Lett. **19**, 1958 (1994).

[2.14] H. A. Haus, D. J. Jones, E. P. Ippen, and W. S. Wong, “Theory of soliton stability in asynchronous modelocking,” IEEE J. Lightwave Technol. **14**, 622 (1996).

[2.15] W. W. Hsiang, C. Y. Lin, M. F. Tien, and Y. C. Lai, “Direct generation of a 10 GHz 816 fs pulse train from an erbium-fiber soliton laser with asynchronous phase modulation,” Opt. Lett. **30**, 2493 (2005).

[2.16] L. F. Mollenauer, J. P. Gordon, and S. G. Evangelides, ‘‘The sliding frequency guiding filter: an improved form of soliton jitter control,’’ Opt. Lett. **17**, 1575 (1992).

[2.17] G. T. Harvey and L. F. Mollenauer, “Harmonically mode-locked fiber ring laser with an internal Fabry-Perot stabilizer for soliton transmission,’’ Opt. Lett. **2**, 107 (1993).

[2.18] W. W. Hsiang, H. C. Chang, and Y. Lai, “Laser dynamics of a 10 GHz 0.55 ps asynchronously harmonic modelocked Er-doped fiber soliton Laser”, IEEE J. Quantum Electron. **3**, 292 (2010).

[2.19] H. G. Weber and M. Nakazawa, “Ultrahigh-Speed Optical

Transmission Technology," (2007).

[2.20] M. Nakazawa, E. Yoshida, and Y. Kimura, "Ultrastable harmonically and regeneratively mode-locked polarization maintaining erbium fiber ring laser," Electron. Lett. **19**, 1603 (1994).

[2.21] H. Takara, S. Kawanishi, and M. Sarawatari, "Stabilization of a modelocked Er-doped fiber laser by suppressing the relaxation oscillation frequency component," Electron. Lett. **4**, 292 (1995).

[2.22] M. Yoshida, K. Kasai, and M. Nakazawa, "Mode-hop-free, optical frequency tunable 40-GHz mode-locked fiber laser," IEEE J. Quantum Electron. **9**, 704 (2007).

[2.23] M. Nakazawa, K. Kasai, and M. Yoshida, "C2h2 absolutely optical frequency-stabilized and 40 GHz repetition rate stabilized regeneratively mode-locked picosecond erbium fiber laser at 1.53 μm," Opt. Lett. **22**, 2641 (2008).

[2.24] M. Nakazawa and M. Yoshida, "Scheme for independently stabilizing the repetition rate and optical frequency of a laser using a regenerative mode-locking technique", Opt. Lett. **33**, 1059 (2008).

[2.25] W. W. Hsiang, C. Lin, N. Sooi, and Y. Lai, “Long-term stabilization of a 10 GHz 0.8 ps asynchronously mode-locked Er-fiber soliton laser by deviation-frequency locking,” Opt. Exp. **5**, 1822 (2006).

Chapter 3

Experimental setup and results

3.1 21GHz asynchronous rational mode-locked Er-fiber soliton laser with stabilization

3.1.1 Experimental setup and component parameters

The system setup of our rational asynchronous mode-locked Er-fiber laser with the feedback control is shown in Fig. 3.1

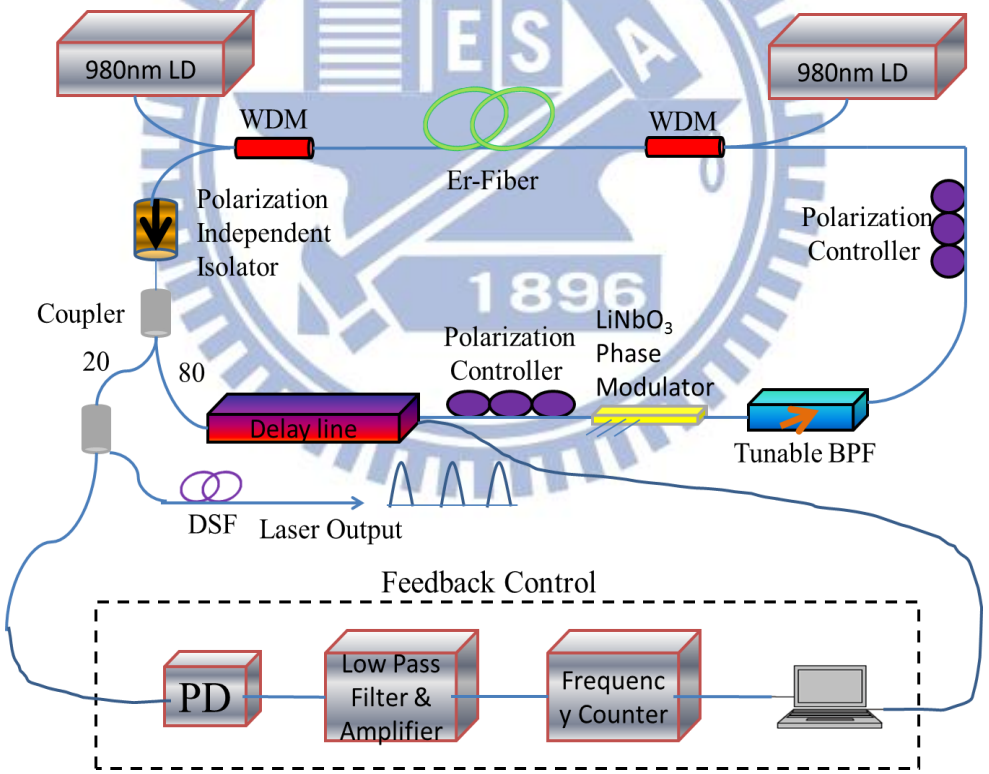

Fig. 3.1 The experimental setup

The schematic diagram of experimental setup consists of two main systems. One is the laser cavity and the other is the feedback control

system. The Er-doped fiber is pumped by two 980 nm laser diodes respectively. The 20/80 coupler divides 80% optical signal into the cavity and 20% into the feedback control system. The feedback control system consists of an optical delay line, a low bandwidth photodetector, a low-pass filter, an amplifier, and a frequency counter. The polarization independent isolator in the cavity is for single direction wave propagation. The phase modulator is to achieve mode-locking by EO effect. The two polarization controllers in the cavity are used to achieve polarization additive pulse mode-locking (PAPM). The devices that have been used in the fiber ring cavity are listed in the Table 3.1.

Table 3.1 Devices in the fiber ring cavity

Device	Specification
Phase modulator	Vπ=4.7 volt @1GHz
980nm pump laser	Maximum output power : 915mA x 1 1164mA x 1
Erbium-doped fiber	~5.5 m
Single mode fiber	~19.5m
Optical delay line	Operating wavelength : 1260-1650 nm Range : 0 ~ 560 ps Resolution : 0.3 μm or 1 fs
Dispersion shifted fiber	~2 m
Coupler	80/20 x 1 ; 95/5 x 1 ; 50/50 x 1
Polarization controller	x 2
Low pass filter	500 Hz to 64000 Hz
Frequency counter	Frequency : DC to 225 MHz
Tunable optical bandpass filter	Bandwidth : 13.5 nm Central wavelength : 1530~1570 nm

3.1.2 Experimental setup and results

From Chapter 2.3, we know how to generate pulse trains of high repetition rates by the method of rational harmonic mode-locking. The pulse trains can reach high quality performance by asynchronous harmonic mode-locking as discussed in Chapter 2.2. Finally, we employ the technique that locks the deviation frequency to control the cavity length for achieving long-term stabilization.

Experimentally, we first set the phase modulation frequency at 7.0128 GHz. Then we detune the frequency to become 7.0128 GHz + $\frac{8\ \mathrm{MHz}}{3}$, where the 8 MHz is the fundamental frequency of cavity. Finally, we can observe the repetition rate frequency at near 21 GHz in RF spectrum. We further detuned the modulation frequency with the smaller amount that closes to near kHz level. The results in the frequency domain and time domain are shown in below:

Fig. 3.2 is the RF spectrum to demonstrate the repetition rate can be up to 21 GHz by the rational harmonic mode-locking with p=3 and the side mode suppression ratio performance is well. The Fig. 3.3 shows high mode-locking quality since the supermode suppression ratio (SMSR) is greater than 60 dB.

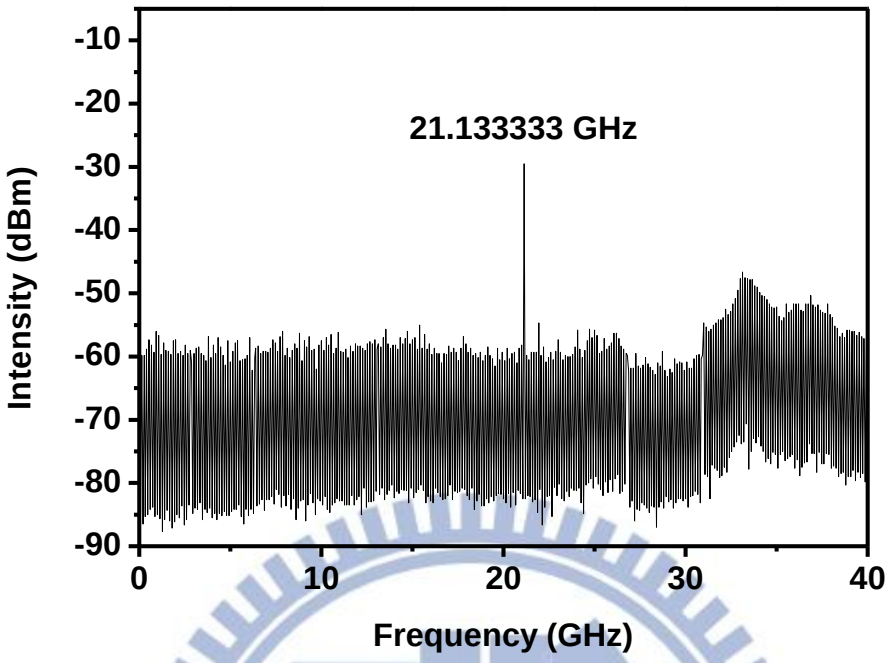

Fig. 3.2 RF spectrum of laser output near 21 GHz with 40 GHz span

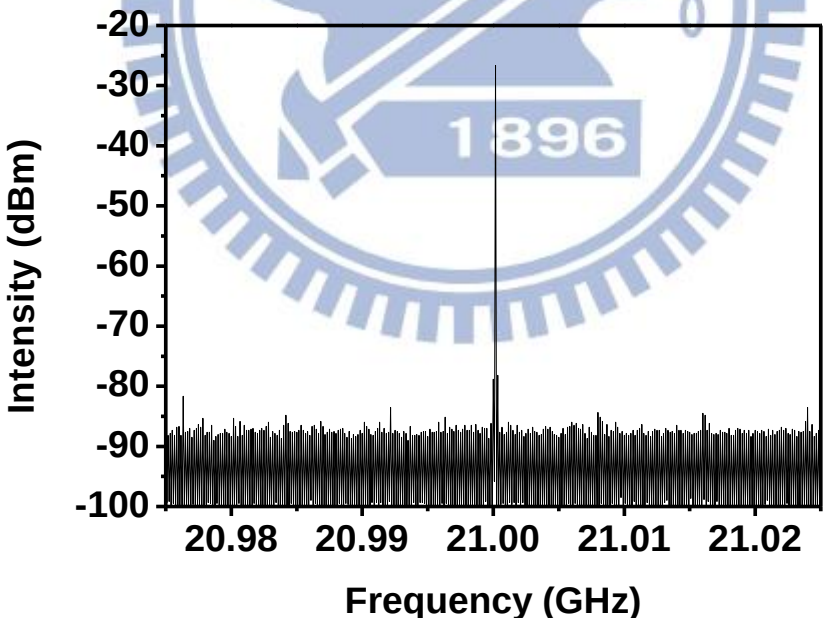

Fig. 3.3 RF spectrum of laser output near 21 GHz with 50 MHz span

Fig. 3.4 show the results of laser outputs under the rational and

asynchronous mode-locked situation. The deviation frequency in this case is ~25 kHz.

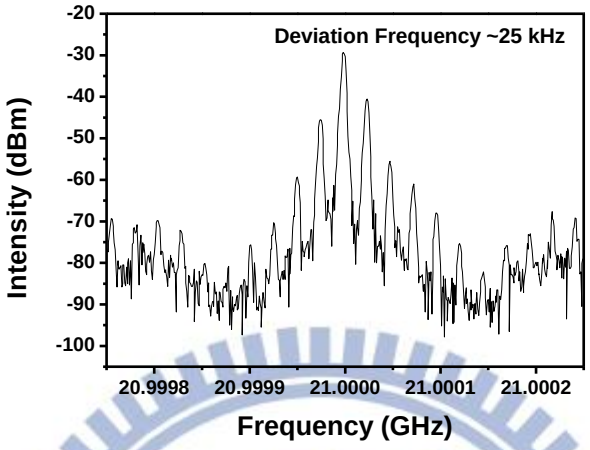

Fig. 3.4 RF spectrum of laser output near 21 GHz with 500 kHz span

In this case, the laser is pumped by bi-directional pumping, and the pumping current is around 850 mA and 800 mA respectively. The optical characteristics and the pulsewidth are shown in Fig. 3.5 and Fig. 3.6 respectively.

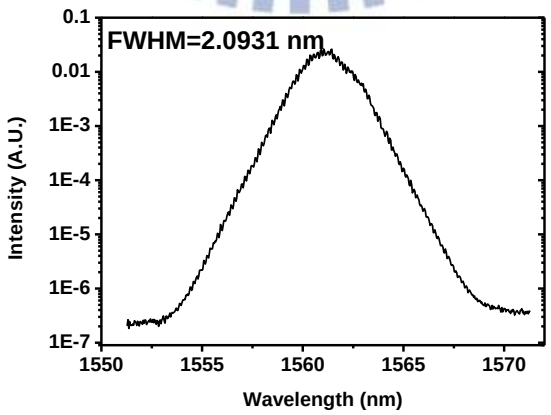

Fig. 3.5 Optical spectrum of the 21GHz rational asynchronous mode-locked Er-fiber soliton laser

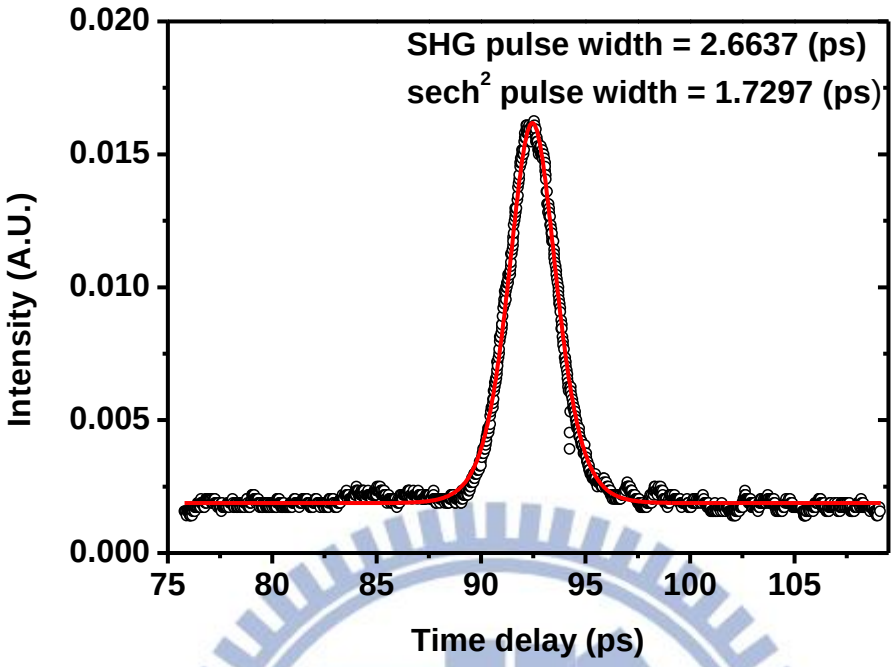

Fig. 3.6 SHG intensity autocorrelation trace (open circles) and the fitting curve (solid curve) of the laser output, assuming sech^2 pulse shape.

Finally, we use the stabilization scheme that is based on controlling the cavity length to lock the deviation frequency at a suitable value [3.1]. Long–term stable mode-locked fiber laser is carried out when the feedback control is turned on. In the 21 GHz rational harmonic mode-locked fiber laser case, the deviation frequency shift can be controlled to be within $\pm 1\text{kHz}$ and the duration of stabilization can be greater than 2000 seconds. The results are shown in Fig.3.7

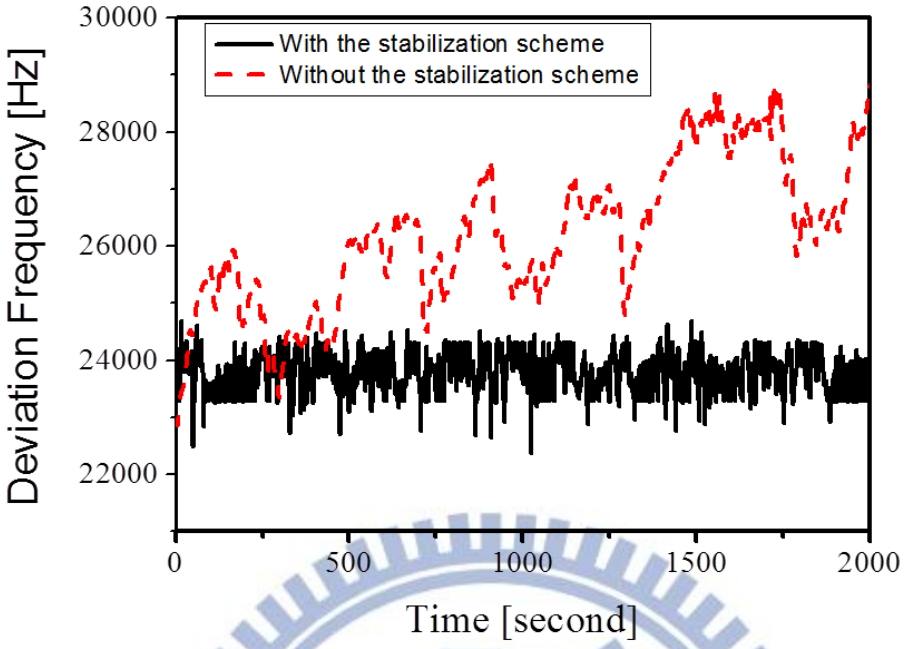

Fig. 3.7 Deviation frequency shift: without the stabilization scheme (red dash line); with the stabilization scheme (black solid line).

Because of the long stable operation duration, we can further measure the laser dynamics in our rational harmonic mode-locked fiber laser system. The results are given in the next section.

3.2 Pulse dynamics of ARHM fiber soliton laser

3.2.1 Periodic pulse timing position and center frequency variation

In the above section, we achieved the high repetition rate by the asynchronous rational harmonic mode-locked method. In this section, we will study the laser dynamics in the ARHM case. We utilize the theory developed in [3.2] to investigate the laser dynamics.

For simplicity we will assume the pulse timing variation is a simple sinusoidal function at the deviation frequency δf. The detected pulse train signals from the fast photodetector can be expressed as:

$$\mathrm{i(t)} = [\mathrm{r(t)} \otimes \mathrm{p(t)}] \otimes \sum_{m=-\infty}^{m=\infty} \delta[t - mT_H + \Delta t_0 \sin(2\pi \delta f_m T_H)] \qquad (3.1)$$

where r(t) is the response function of fast photodetector, p(t) is the pulse intensity, T_H is the period of the cavity harmonic, Δt_0 is the half peak-to-peak displacement of sinusoidal pulse timing variation, $\delta[.]$ is the Dirac's delta function, and $\otimes$ is the operation of convolution. The Fourier transform of the photocurrent i(t) can be expressed to be:

$$\mathrm{F\{i(t)\}} = \mathrm{F\{r(t)\}} * \mathrm{F\{p(t)\}} * \mathrm{F}\{\sum_{m=-\infty}^{m=\infty} \delta[.]\} \qquad (3.2)$$

$$(\delta[.] = \delta[t - mT_H + \Delta t_0 \sin(2\pi * \delta f * mT_H)])$$

$$i(\omega) = r(\omega) * p(\omega) * \sum_{n=-\infty}^{n=\infty} J_n(\omega \Delta t_0) \sum_{m=-\infty}^{m=\infty} \delta(\omega - 2\pi m f_H - 2\pi n \delta f) \quad (3.3)$$

where $r(\omega)$ and $p(\omega)$ are the Fourier transforms of the response function of fast photodetector and the pulse intensity respectively, and $J_n(.)$ is the Bessel function of the first kind of order n. As said above, the pulse trains with a sinusoidal timing variation in the time domain can be converted to the frequency domain like a comb as show in Fig. 3.8. From equation (3.3), the sinusoidal timing variation is converted to amplitudes of $J_n(\omega \Delta t_0)$ in the frequency domain, which is spaced equally by the deviation frequency δf around the harmonic mode ($m f_H$). Because I(ω) is proportional to $|J_n(\omega \Delta t_0)|^2$, we can estimate the Δt_0 from the power ratio of the 0th (the cavity harmonic frequency) and 1st (the modulation frequency) spectral peaks. It is written as:

$$\Delta = \left| \frac{J_0(2\pi m f_H \Delta t_0)}{J_1[2\pi(m f_H + \delta f)\Delta t_0]} \right|^2$$

$$\rightarrow I_A - I_B = 10 \log_{10} \Delta$$

$$= 20 \log_{10}\left(\left| \frac{J_0(2\pi m f_H \Delta t_0)}{J_1[2\pi(m f_H + \delta f)\Delta t_0]} \right| \right)$$

$$\approx 20 \log_{10}\left(\left| \frac{J_0(2\pi m f_H \Delta t_0)}{J_1[2\pi(m f_H)\Delta t_0]} \right| \right) \quad (3.4)$$

We can use the equation (3.4) to calculate the pulse timing variation for the asynchronous rational harmonic mode-locked fiber lasers.

For comparing with the experimental data, we will use the approximate analytic formula derived in [3.2], which is given below:

$$\Delta\omega = \frac{M}{R}\frac{1}{\sqrt{1+\left(\frac{4d_r}{3\tau^2\omega_m R}\right)^2}} \tag{3.5}$$

$$\Delta t_0 = \frac{2d_i M}{\omega_m R^2}\frac{1}{\sqrt{1+\left(\frac{4d_r}{3\tau^2\omega_m R}\right)^2}} \tag{3.6}$$

Also from [3.2], we know the phase difference between the pulse timing variation and the pulse center frequency variation is $\frac{\pi}{2}$. The pulse center frequency variation can be identified by comparing the timing variation before and after a propagation length of SMF-28. The formula is shown as below:

$$\begin{aligned}\Delta t_{total} &= \Delta t_0 \sin(RT) + \Delta\lambda DL\cos(RT)\\ &= \sqrt{(\Delta t_0)^2 + (\Delta\lambda DL)^2}\sin(RT+\phi)\\ &= \Delta t_1 \sin(RT+\phi)\end{aligned} \tag{3.7}$$

where the term $\Delta\lambda DL\cos(RT)$ is the extra pulse timing variation resulted from the dispersion of external SMF-28. Equation (3.7) can be derived to get the equation (3.8)

$$\Delta\lambda = \frac{\sqrt{\Delta t_1^2 - \Delta t_0^2}}{DL} \tag{3.8}$$

where Δt_1 and Δt_0 are the timing variations after and before SMF-28 respectively.

The RF spectra with span 500 kHz are shown in the Fig. 3.8, Fig. 3.9, Fig. 3.10, and Fig. 3.11. The pulse trains propagate through the external section of SMF-28 with the length of 0m, 200m, 300m, and 500m respectively.

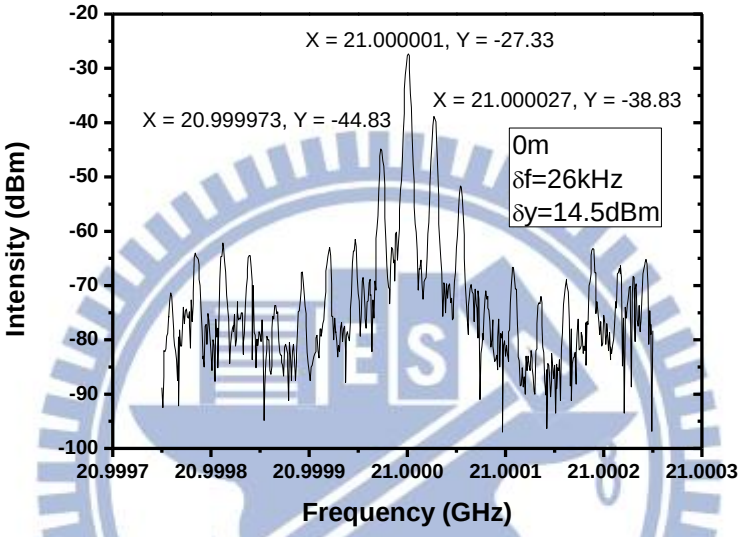

Fig. 3.8 RF spectrum at 21 GHz with 0 m SMF 28 fiber

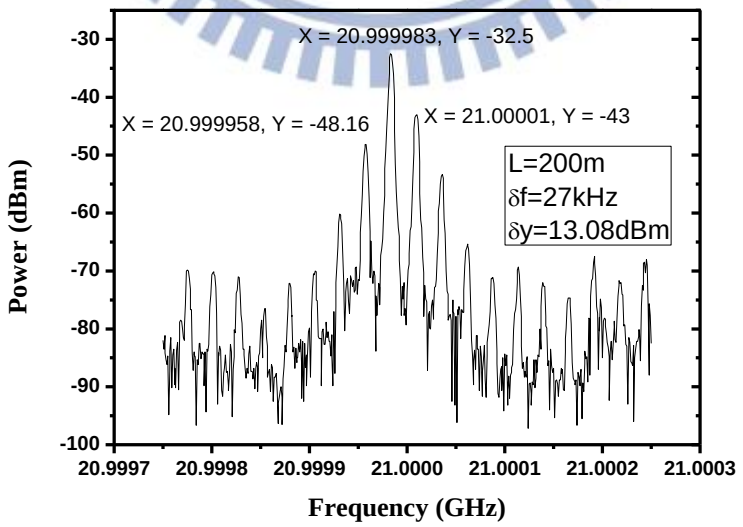

Fig. 3.9 RF spectrum at 21 GHz with 200 m SMF 28 fiber

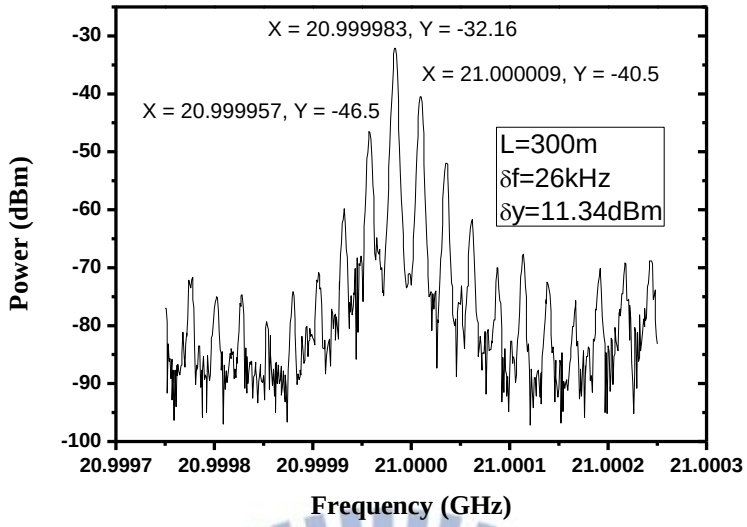

Fig. 3.10 RF spectrum near 21 GHz with 300 m SMF 28 fiber

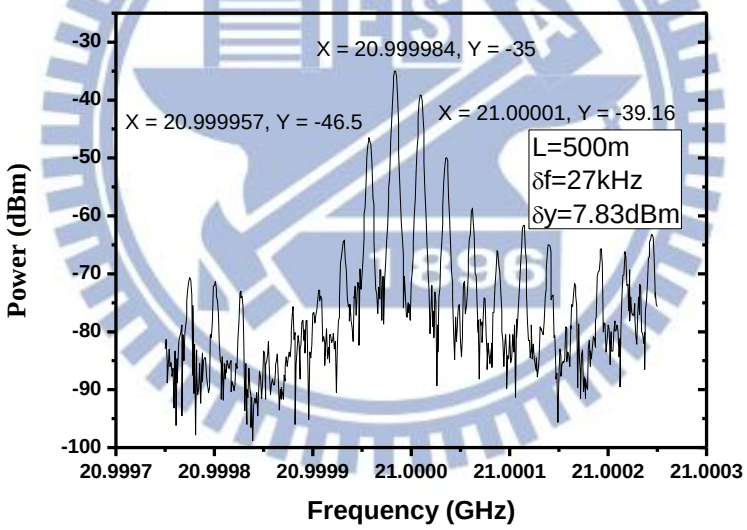

Fig. 3.11 RF spectrum near 21 GHz with 500 m SMF 28 fiber

According to these data and equation (3.4), the relation between the external section of SMF-28 and pulse timing variation is shown in Fig. 3.12

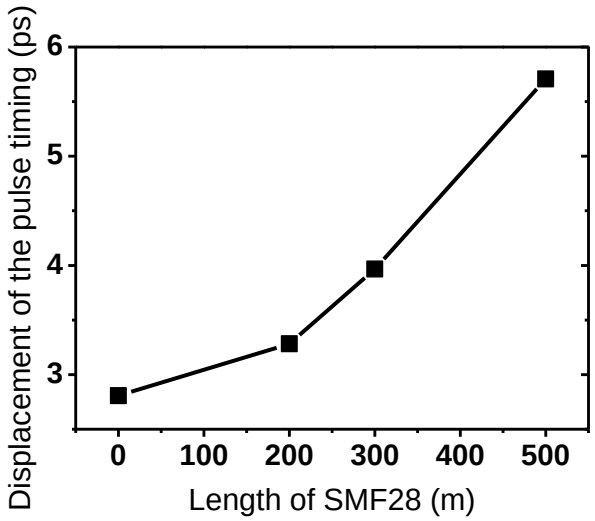

Fig. 3.12 Measurement of the net pulse timing variation versus the length of the SMF-28 fiber.

Furthermore, we take the periodic pulse timing position variation and the parameter of SMF-28 into the question (3.8) to get the pulse center frequency variation. The experimental and calculated results are listed in Table 3.2.

Table 3.2 Ratios of the RF intensity and the estimated wavelength variation

SMF 28 Length (m)	**Ia-Ib (dBm)**	**Δt (ps)**	**Δλ(nm)**
0m	**14.5**	**2.80596**	
200m	**13.08**	**3.28278**	**0.5011434**
300m	**11.34**	**3.96577**	**0.5495068**
500m	**7.83**	**5.7068**	**0.584626**

Finally, the average pulse center frequency variation of $\Delta\lambda$ is 0.545092 nm. We have measured and saved the RF spectra for different lengths of SMF-28 fiber and calculated the values of the periodic pulse timing position variation. These results provide us to estimate the effective modulation depth in this particular case. We find that the modulation depth in the asynchronous rational harmonic mode-locked fiber laser is mainly contributed by the higher order harmonics from the electronic amplifier.

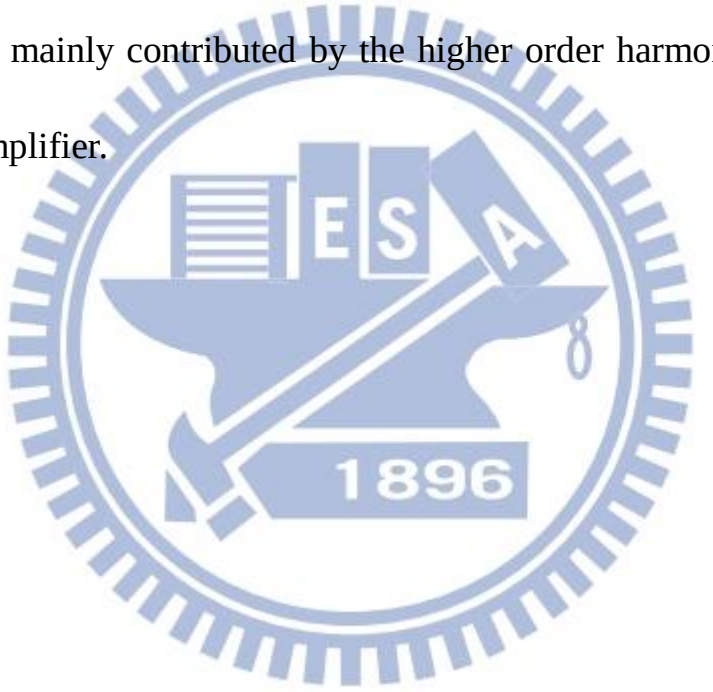

3.2.2 Determination of the effective modulation depth

The journal paper [3.3] indicated that the rational harmonic mode-locking with a phase modulator is mainly due to the contributions of higher order harmonics from the amplified electrical driving signal. In this section, we will use another way to determine the conclusion of [3.1]. Based on the section 3.3.1 results, we can further use these results to calculate the effective modulation depth of the mode-locked fiber laser. In this section, we set two different experimental cases to enhance the accuracy of experiments. The first one is the rational harmonic mode-locking and the other is the harmonic mode-locking. We detune the operation parameters to let their effective modulation strength get close. The equation (3.9) is derived from equation (3.6) and is shown below:

$$M = \frac{\Delta t \omega_m R^2}{2 d_i} \sqrt{1 + \left(\frac{4 d_r}{3 \tau^2 \omega_m R}\right)^2} \qquad (3.9)$$

Figure 3.13 is the RF spectrum with no external section of SMF-28 in the rational harmonic mode-locked case. The deviation frequency is ~26 kHz and the power difference of the 0th (the cavity harmonic frequency) and 1st (the modulation frequency) order spectral peaks is 14.5 dB. This

is shown in Fig. 3.13.

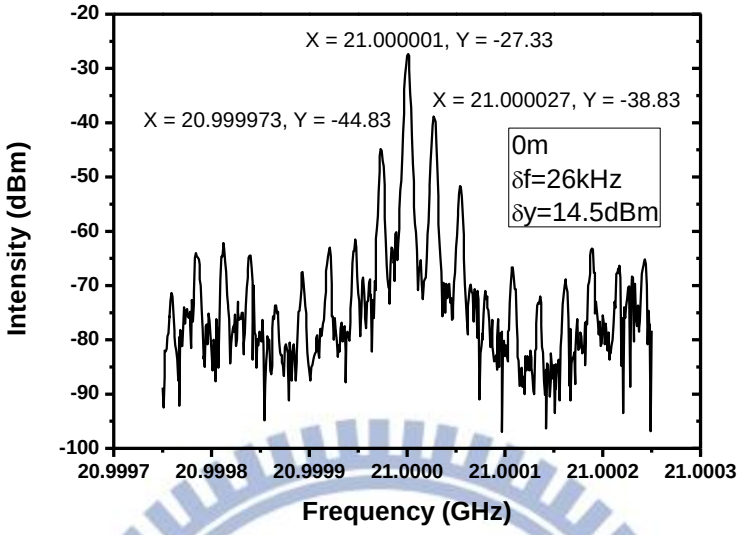

Fig. 3.13 RF spectrum at 21 GHz with 0 m SMF 28 fiber

The second-harmonic generation (SHG) intensity autocorrelation trace is shown in Fig. 3.14 by open circles. With the assumption of $sech^2$ pulse shape, the solid line in Fig 3.14 is the fitting curve of the SHG intensity autocorrelation trace and the pulsewidth is 1.7297 ps.

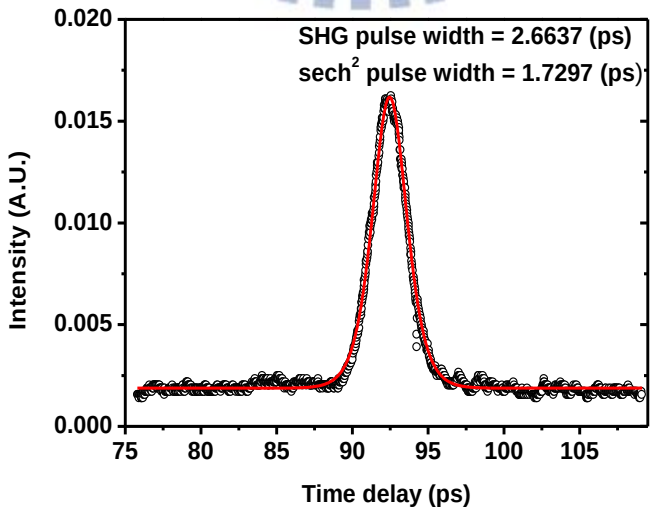

Fig. 3.14 SHG intensity autocorrelation trace (open circles) and the fitting curve (solid

curve) of the laser output, assuming sech2 pulse shape.

The simulation parameters used here are listed in Table 3.3

Table 3.3 Simulation parameters in rational harmonic mode-locking

The simulation parameters (Rational harmonic mode-locking)	
δf	26 kHz
f_R	8 MHz
f_m	21 GHz
d_r	0.05
d_i	0.2
τ	1.7297 ps
Δ t	2.80596 ps

These parameters are normalized by a time units of 0.5 ps, which is near the laser pulsewidth. The value of d_r is determined from the filter bandwidth (13.5 nm) and the value of d_i is determined from the estimated cavity average dispersion (-4.1ps^2/km) as we well as the cavity length (25m). After substituting these parameters in equation (3.9), we get the effective modulation depth (M) to be 0.091917.

The comparative case is the harmonic mode-locking. The RF spectrum and pulsewidth profiles are given in Fig. 3.15 and Fig. 3.16 respectively.

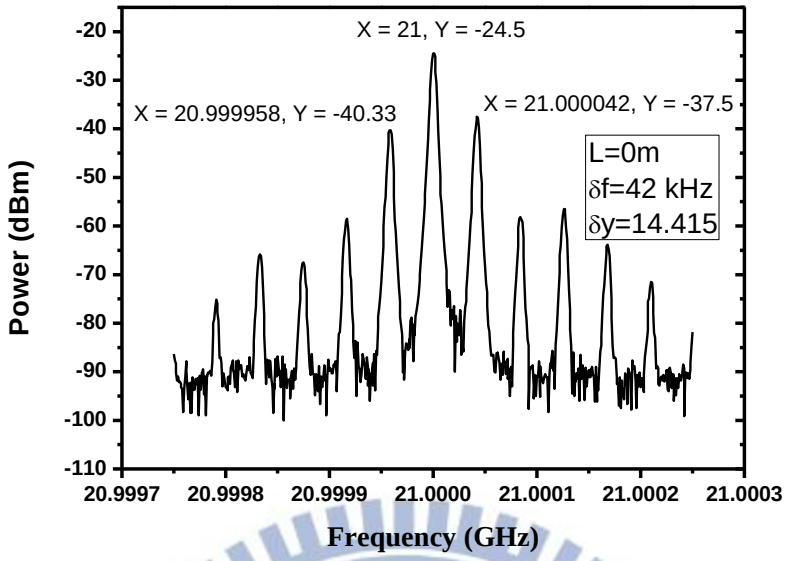

Fig. 3.15 RF spectrum at 21 GHz with 0 m SMF 28 fiber

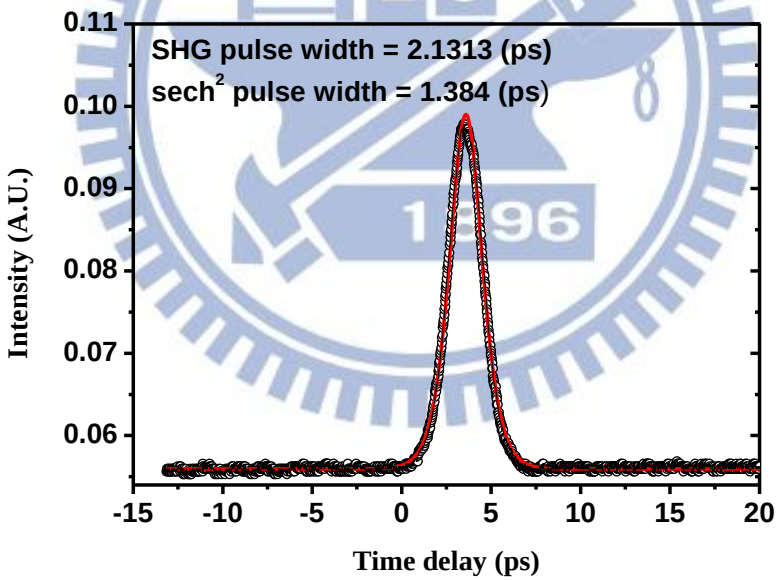

Fig. 3.16 SHG intensity autocorrelation trace (open circles) and the fitting curve (solid curve) of the laser output, assuming sech2 pulse shape.

The simulation parameters used are listed in Table 3.4

Table 3.4 Simulation parameters in harmonic mode-locking

The simulation parameters (Harmonic mode-locking)	
δf	42 kHz
f_R	8 MHz
f_m	21 GHz
d_r	0.05
d_i	0.2
τ	1.384 ps
Δ t	2.8326 ps

After substituting these parameters in equation (3.9), we get the effective modulation depth (M) is 0.241585. And a comparison table is given below.

Table 3.5 Comparison table between harmonic mode-locking and rational harmonic mode-locking

	Harmonic mode-locking	**Rational harmonic mode-locking**
Delta dBm	14.415 dBm	14.5 dBm
Timing variation	2.8326 ps	2.80596 ps
Deviation frequency	42 kHz	26 kHz
Pulsewidth (sech^2 shaping)	1.384 ps	1.7297 ps
Effective modulation depth	M: 0.241585	M: 0.091917
Effective modulation power	1.16037 dBm	-7.23313 dBm

The effective modulation can be related to the driving power of the modulator with the dBm unit. The formula is given below:

$$\text{M (dBm)} = 10 * \log_{10}\left[\left(\frac{M*4.7}{\pi}\right)^2 * \frac{1}{2*50} * \frac{1}{1\,mW}\right] \quad (3.10)$$

The experimental modulation power injected into the modulator is ~14 dBm in the harmonic mode-locking and >5.34 dBm in the rational harmonic mode-locking respectively. The difference between the experimental values and theoretical ones may be caused by the noise disturbances from the laser system. However, it matches the result that broad pulsewidth with low modulation depth in rational harmonic mode-locking by referring to reports of C. Wu and N. K. Dutta [3.6]. Base on the laser dynamics of asynchronous harmonic mode-locking, we calculate a lower modulation depth in the rational harmonic mode-locking case. This is another way to demonstrate the rational harmonic mode-locking with a phase modulator is mainly due to the contributions of the higher order harmonic terms from the amplified electrical driving signal.

3.3 33GHz asynchronous rational harmonic mode-locked Er-fiber soliton laser

In this section, we improve our laser system to operate at 33 GHz asynchronous rational harmonic mode-locking. In the frequency domain we show the results of RF spectrum in the Fig 3.17, Fig. 3.18 and Fig. 3.19.

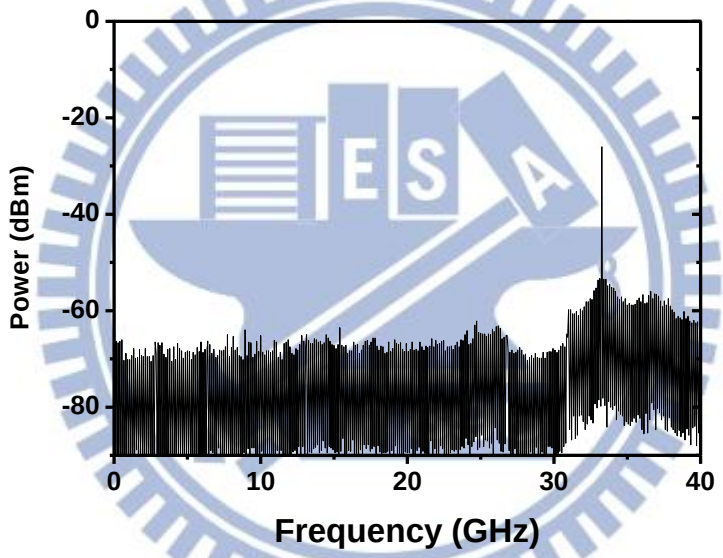

Fig. 3.17 RF spectrum of laser output near 33 GHz with 40 GHz span

As shown in Fig. 3.17 we observe certainly that the repetition rate of 33 GHz has been achieved, when the modulation frequency is operated at 11 GHz with p=3 and the sidemode suppression ratio performance is very well. The bandwidth of the RF amplifier we used is 26.5 GHz.

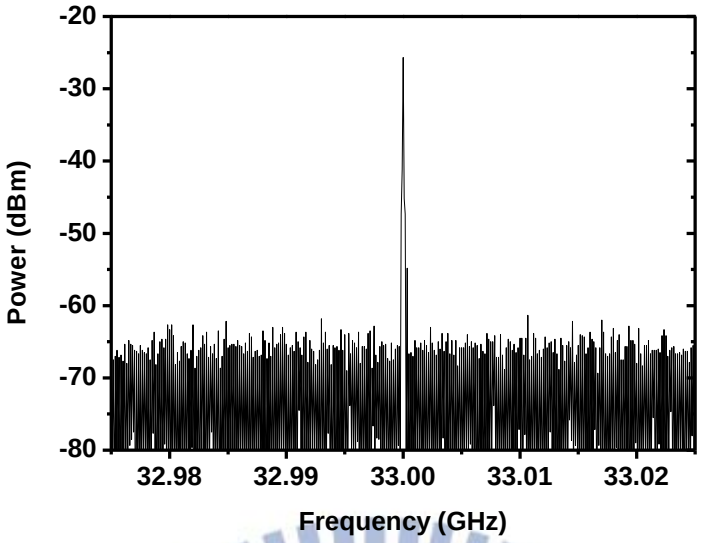

Fig. 3.18 RF spectrum of laser output near 33 GHz with 50 MHz span

As shown in the Fig. 3.18 the supermode noise suppression is suppressed very well.

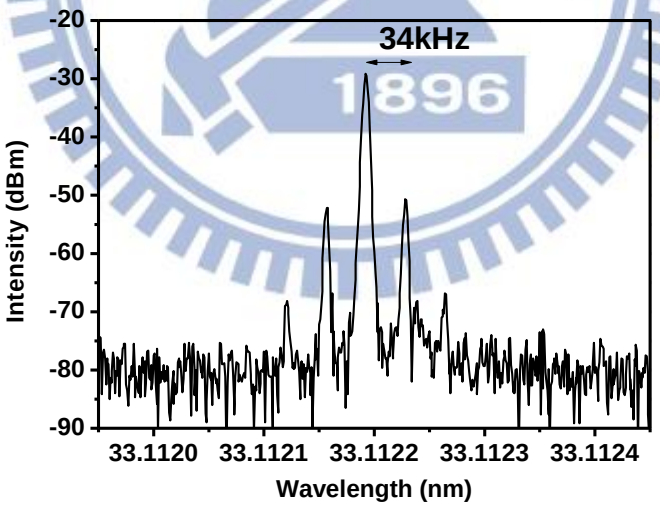

Fig. 3.19 RF spectrum of laser output near 33 GHz with 500 kHz span

Fig. 3.20 shows the optical spectrum of the laser output. The full-width half-maximum (FWHM) bandwidth of the optical spectrum is 1.28 nm.

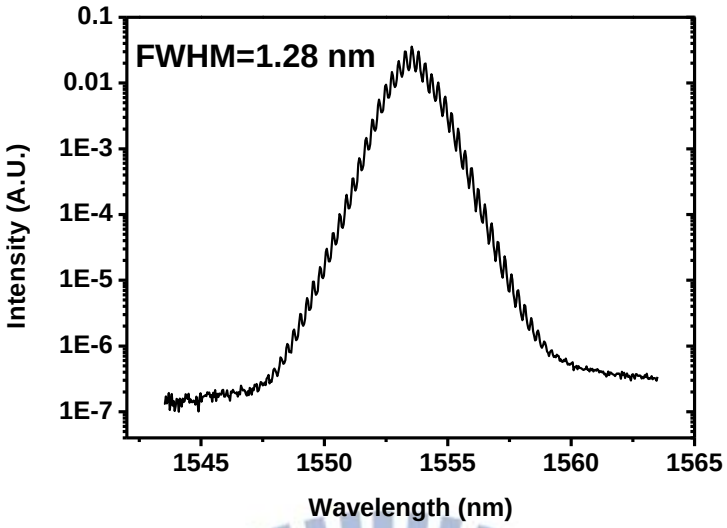

Fig. 3.20 Optical spectrum of the 33GHz asynchronous rational mode-locked Er-fiber soliton laser

Finally, the pulse profile is shown in Fig. 3.21 and with the assumption of $sech^2$ pulse shape, indicating that the pulsewidth is 2.5477 (ps).

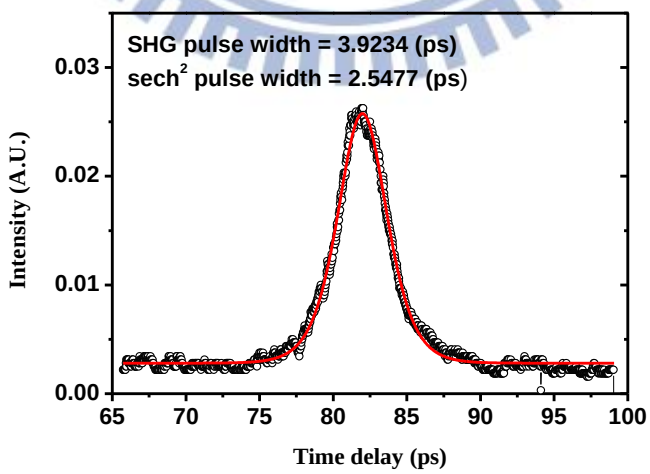

Fig. 3.21 SHG intensity autocorrelation trace (open circles) and the fitting curve (solid curve) of the laser output, assuming sech2 pulse shape.

3.4 New synchronous harmonic mode-locked operation state

When we measured the laser dynamics as mentioned above, we also found a new mode-locked fiber laser operation state. This mode-locked situation exhibits spectral peaks at a larger deviation frequency than the deviation frequency of ARHML in our knowledge. This new state also exhibits high SMSR as shown in Fig. 3.23 and Fig. 3.29. The allowed region of the deviation frequency is very small so that it can provide us an obvious operating point (i.e. the laser gets mode-locked perfectly once it enters this large deviation frequency region). Finally, we can also employ the long-term stabilization scheme based on the deviation-frequency locking to stabilize the laser. We also show that both the harmonic mode-locked case and the rational harmonic mode-locked case can be operated in this new state.

We first demonstrate the harmonic mode-locked fiber laser with a large deviation frequency. The experimental setup is the same as in Fig. 3.1. The results in this case include the RF spectrum, pulsewidth profile, optical spectrum and laser stabilization. The experimental parameters are listed in Table 3.6.

Table3.6 Parameters for the new harmonic mode-locked state

Parameters of harmonic mode-locking	
980 nm pump	L:850 mA ; R:800 mA
Repetition rate	39.997017 GHz
Synthesizer power	-7 dBm
Results	
Optical center frequency	1559.32 nm
Optical spectrum bandwidth	2.0713 nm
Pulsewidth	1.8412 ps
Output power	27 mW
SMSR	>55 dB
Deviation frequency	189 kHz

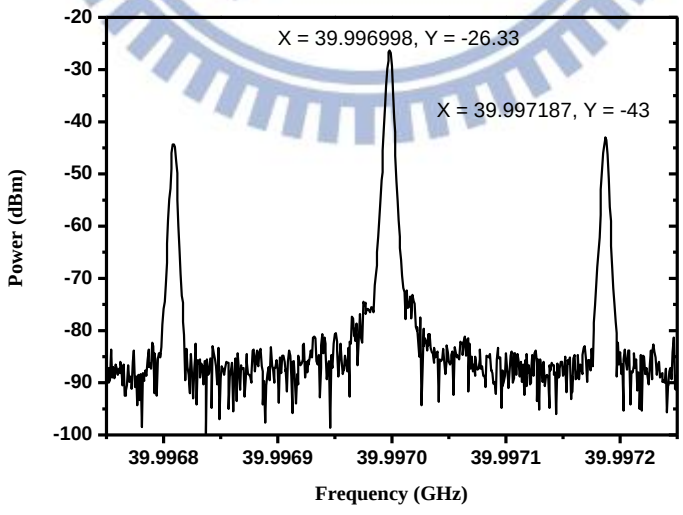

Fig. 3.22 RF spectrum at 40 GHz in with 500 kHz span

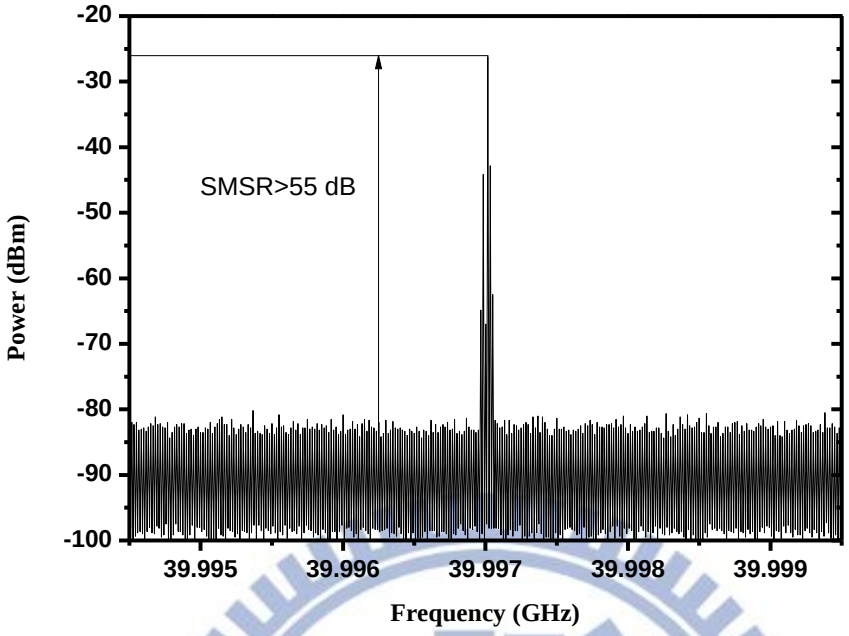

Fig. 3.23 RF spectrum at 40 GHz with 50 MHz span and SMSR > 55 dB

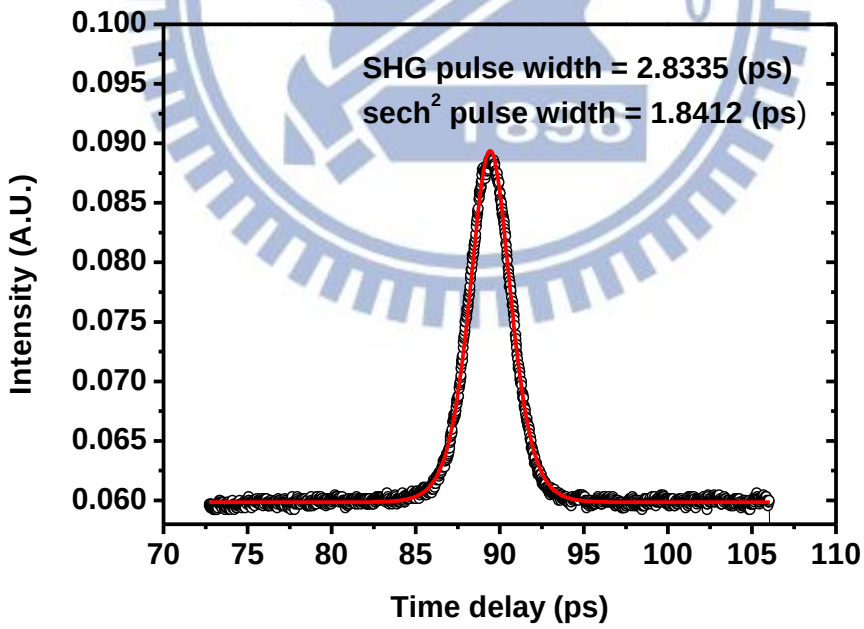

Fig. 3.24 SHG intensity autocorrelation trace (open circles) and the fitting curve (solid curve) of the laser output, assuming sech2 pulse shape.

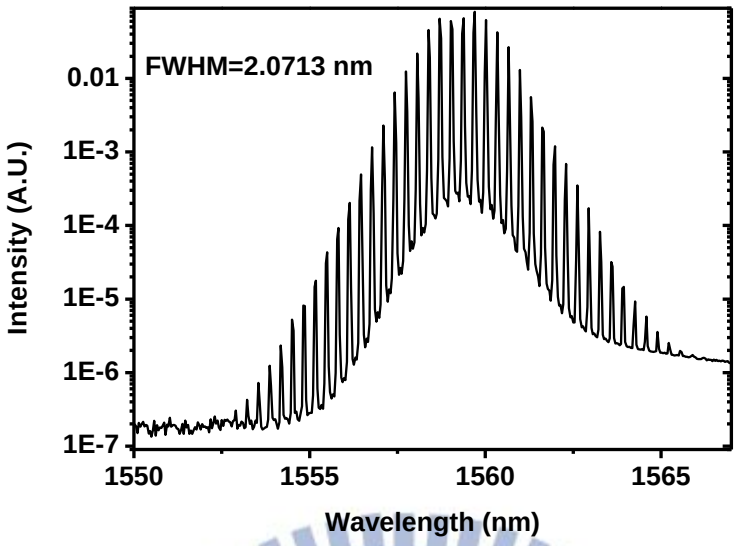

Fig. 3.25 Optical spectrum of the 40GHz harmonic mode-locked Er-fiber soliton laser

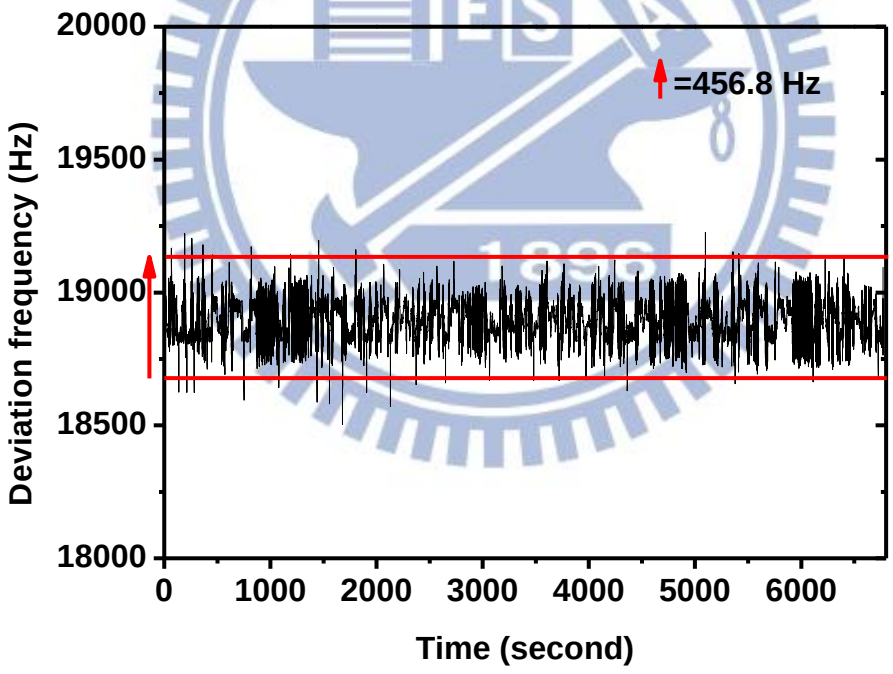

Fig. 3.26 The deviation frequency shift with duration time of stabilization

We then demonstrate the rational harmonic mode-locked fiber laser with large deviation frequency. The results in this case include the RF spectrum, pulsewidth profile and optical spectrum. The experimental

parameters are listed in table 3.7.

Table3.7 Parameters in new harmonic mode-locked state

Parameters of rational harmonic mode-locking	
980 nm pump	L:850 mA ; R:800 mA
Modulation frequency	13.308938 GHz
Synthesizer power	3 dBm
Results	
Repetition rate	39.928 GHz
Optical center frequency	1559.12 nm
Optical spectrum bandwidth	1.638 nm
Pulsewidth	1.9946 ps
Output power	27 mW
SMSR	~60 dB
Deviation frequency	183 kHz

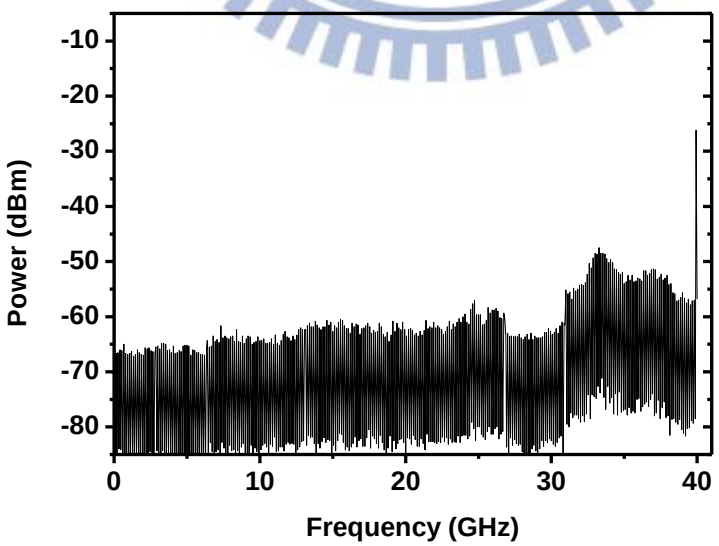

Fig. 3.27 RF spectrum at near 40 GHz with 40 GHz span

In the RF spectrum with span 40 GHz, one can see that the unwanted harmonic sidemodes are suppressed very well.

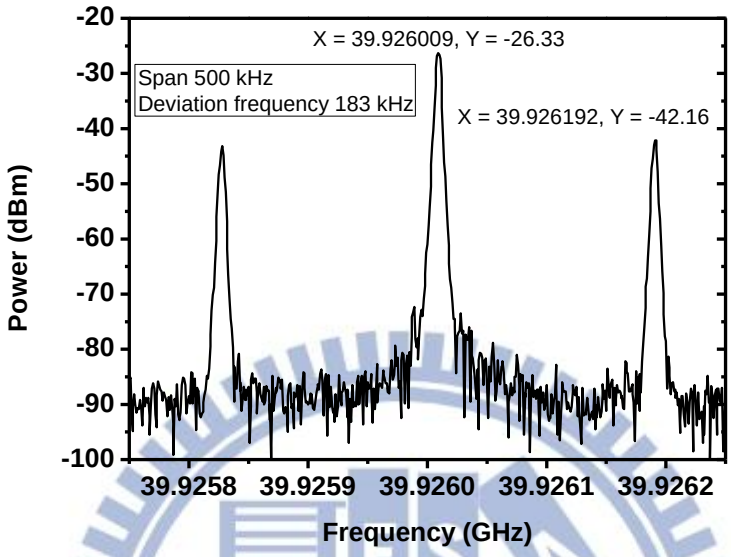

Fig. 3.28 RF spectrum at near 40 GHz in with 500 kHz span

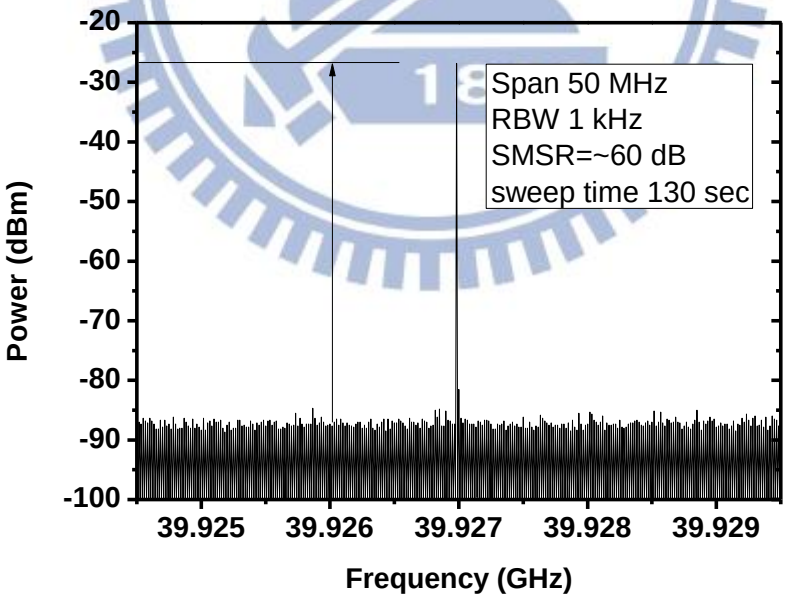

Fig. 3.29 RF spectrum at near 40 GHz with 50 MHz span and SMSR ≈ 60 dB

In the RF spectrum with span 50 MHz, one can see that the supermode noises are also suppressed very well.

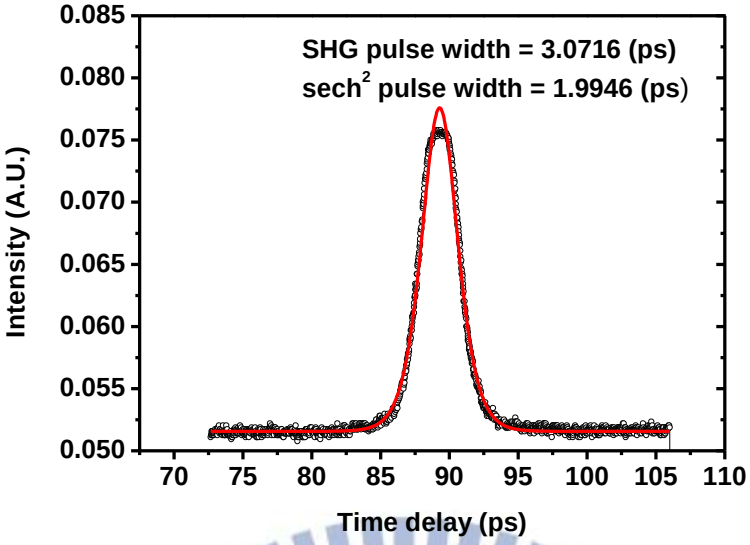

Fig. 3.30 SHG intensity autocorrelation trace (open circles) and the fitting curve (solid curve) of the laser output, assuming sech2 pulse shape.

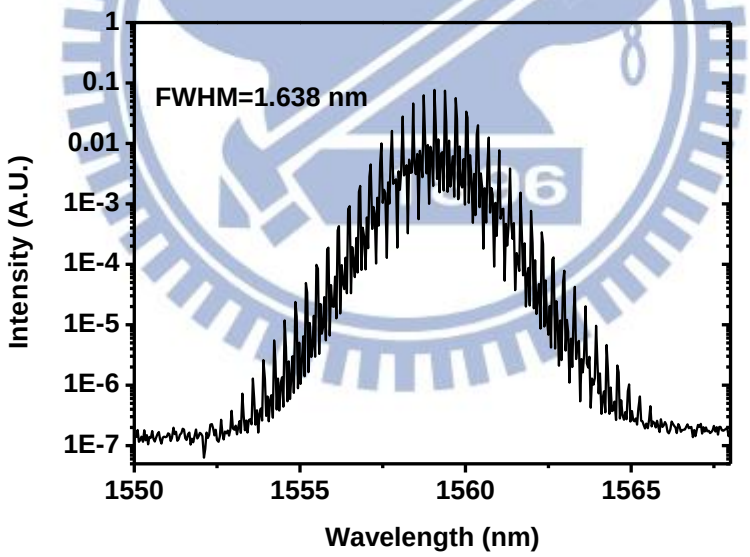

Fig. 3.31 Optical spectrum of the 40GHz rational harmonic mode-locked Er-fiber soliton laser

Even though this situation is quite similar to asynchronous mode-locking, the observed optical spectrum exhibits clear mode spacing

and this operation mode is reached by setting the modulation frequency very close to the harmonic frequency of cavity. These characteristics indicate that this new mode-locked state should be close to synchronous mode-locking rather than asynchronous mode-locking. So we start to design a series of experiments to check if this state is asynchronous mode-locking or not. These experiments are given below.

First, we measure the oscillation frequency from the low frequency spectrum of the pulse train and the result is shown in Fig. 3.32.

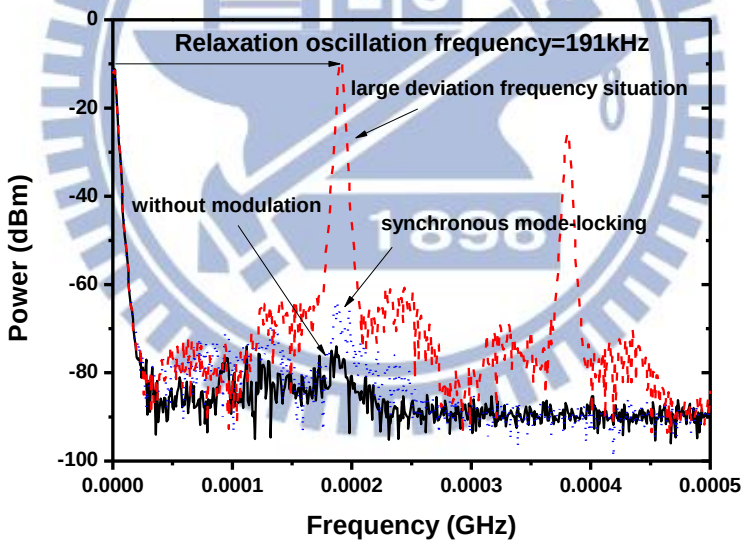

Fig. 3.32 Low frequency spectrum of the output pulse train. Large deviation frequency situation (red dash line), synchronous situation (blue dot line) and no modulation signal situation (black solid line).

It is easy to see that the amplitude of oscillation frequency in large

deviation frequency mode-locking is higher than the other states. Based on this result, we expect the deviation frequency is induced by gain dynamics instead of asynchronous mode-locking.

Secondly, we want to know if the oscillation frequency is really induced by the gain dynamics or not. We change the pumping power to record the difference of the oscillation frequency. The experimental result is plotted versus the optical power of the autocorrelator port as shown in the Fig.3.33, a linear dependence is clearly seen.

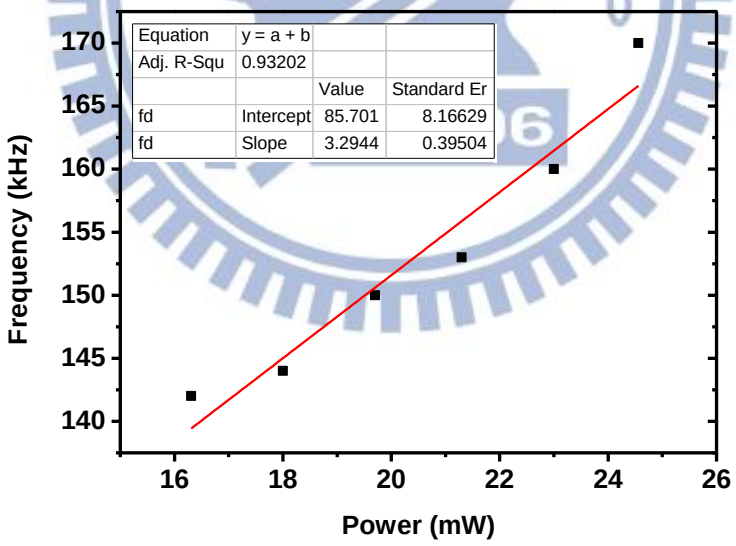

Fig. 3.33 Linear relation between the optical power of the autocorrelator port and the deviation frequency of the spectral side peaks.

Based on this result, we can conclude that the deviation frequency is proportional to the pumping power.

Finally, we use the sampling scope to check directly if this state is asynchronous mode-locking or not. The sampling scope has two ports, one is the signal port and the other is the trigger port. In the synchronous mode-locked case, the trigger port signal from the synthesizer can correctly trigger the signal of the laser output. On the contrary, the signal of the laser output is with slow timing variation in the asynchronous mode-locking case so that it cannot be triggered correctly. It means that if the triggered process can be carried out successfully, then it is not the asynchronous mode-locking.

The obtained results are given in Fig. 3.34, Fig. 3.35 and Fig. 3.36 with the synchronous mode-locking, large deviation frequency mode-locking and asynchronous mode-locking cases respectively.

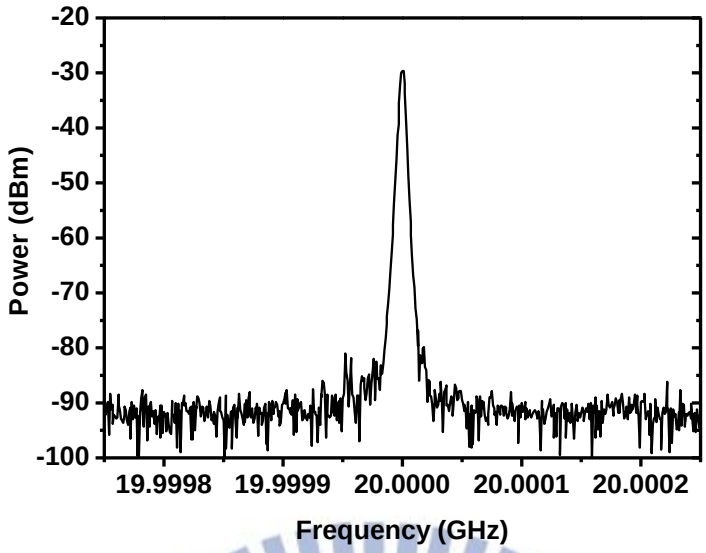

Fig. 3.34(a) RF spectrum in synchronous mode-locking at near 20 GHz with 500 kHz span

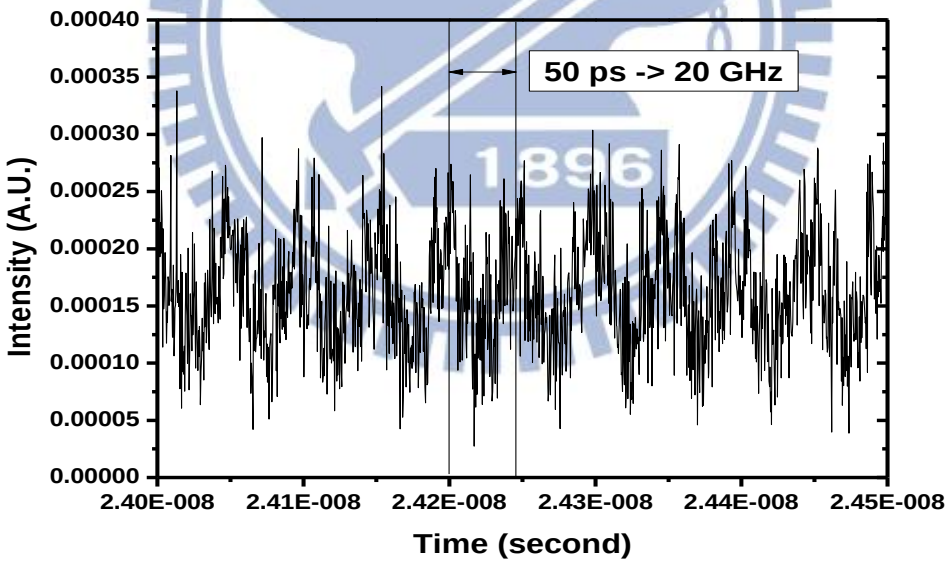

Fig. 3.34(b) Synchronous mode-locked pulse trains by the fast sampling oscilloscope

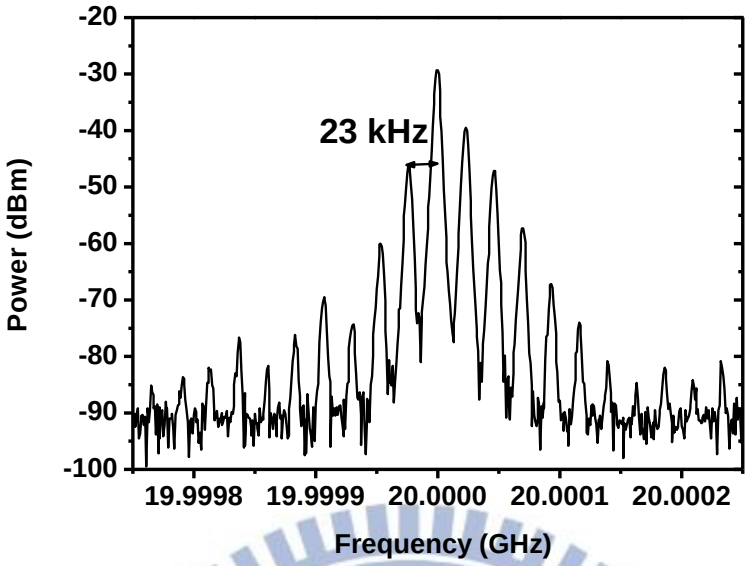

Fig. 3.35(a) RF spectrum in asynchronous mode-locking at near 20 GHz with 500 kHz span

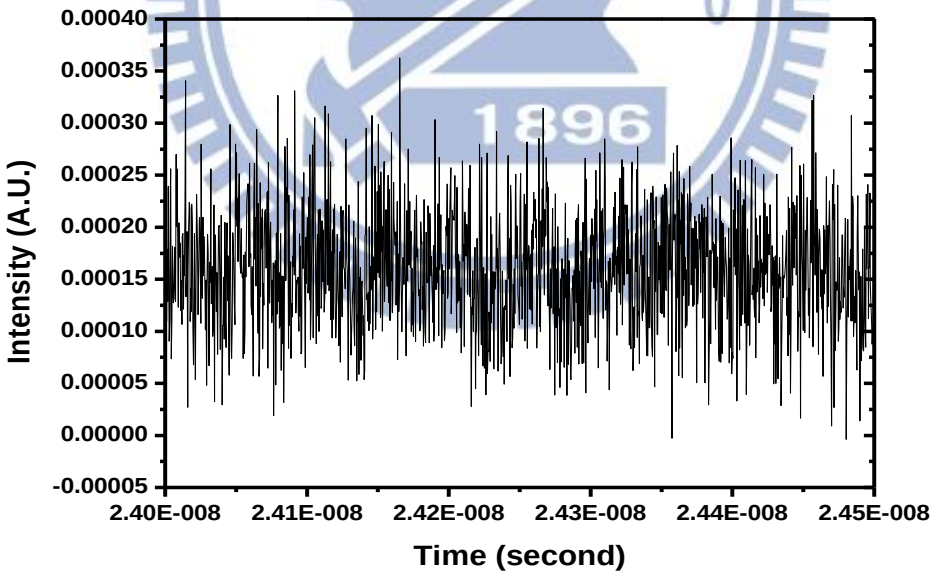

Fig. 3.35(b) Asynchronous mode-locked pulse trains by the fast sampling oscilloscope

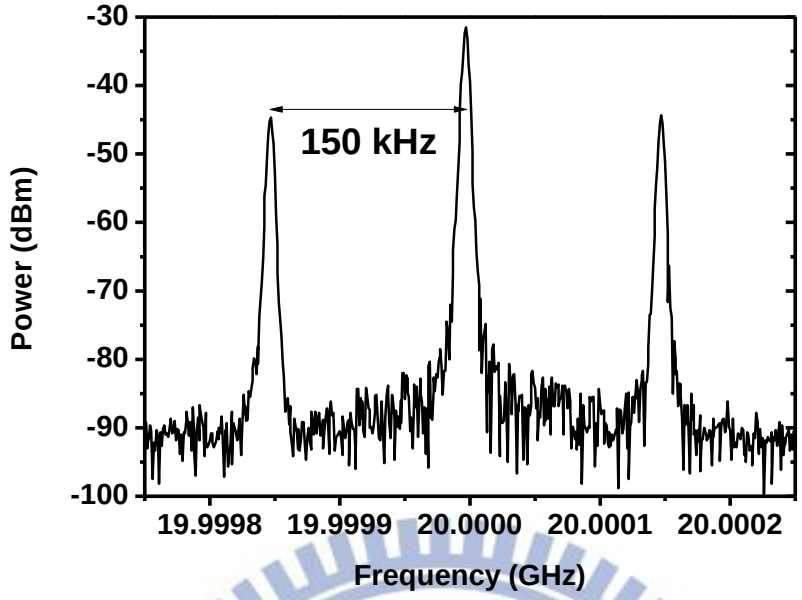

Fig. 3.36(a) RF spectrum in large deviation frequency mode-locking at near 20 GHz with 500 kHz span

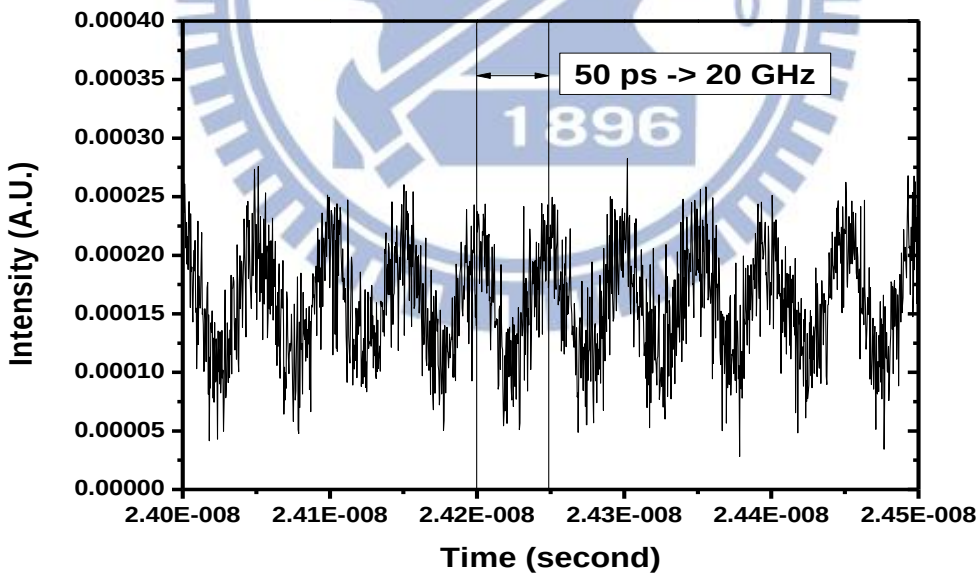

Fig. 3.36(b) Large deviation frequency mode-locked pulse trains by the fast sampling oscilloscope

It is easy to see that the pulse trains can be observed and the period of pulse trains can be calculated in the Fig. 3.34 and Fig. 3.36. On the contrary, in Fig. 3.35, the asynchronous mode-locked pulse trains cannot be triggered as we expected. So this is the direct way to prove that the new mode-locked state is synchronous mode-locking instead of asynchronous mode-locking.

Reference

[3.1] W. W. Hsiang, C. Y. Lin, N. Sooi and Y. Lai, “Long-term stabilization of a 10 GHz 0.8 ps asynchronously mode-locked Er-fiber soliton laser by deviation-frequency locking,” Opt. Express **5**, 1822 (2006).

[3.2] W. W. Hsiang, H. C. Chang, and Y. Lai, “Laser dynamics of a 10 GHz 0.55 ps asynchronously harmonic modelocked Er-doped fiber soliton Laser”, IEEE J. Quantum Electron. **3**, 292 (2010).

[3.3] S. Yang and X. Bao, “Rational harmonic mode-locking in a phase modulated fiber laser,” IEEE Photon. Technol. Lett. **12**, 1332 (2006).

[3.4] S. Yang, J Cameron and X. Bao, “Stabilized phase-modulated rational harmonic mode-locking soliton fiber laser,” IEEE Photon. Technol. Lett. **6**, 393 (2007).

[3.5] H. Takara, S. Kawanishi and M. Saruwatari, “Stabilization of a modelocked Er-doped fiber laser by suppressing the relaxation oscillation frequency component,” Electronics Lett. **4**, 292 (1995)

[3.6] C. Wu and N. K. Dutta, “High-repetition-rate optical pulse generation using a rational harmonic mode-locked fiber laser,”

IEEE J. Quantum Electron. **2**, 145 (2000).

Chapter 4

Conclusions

4.1 Summary of achievements

In summary, we have demonstrated successfully the following main achievements.

First, we have successfully achieved the long-term stabilization of a 21 GHz asynchronous rational harmonic mode-locked Er-doped fiber soliton laser by the deviation-frequency locking method. The duration of stabilization can last longer than 2000 seconds and the deviation frequency shift can be controlled to be within ± 1 kHz.

Second, based on the first achievement, we have successfully calibrated the laser dynamics of the asynchronous rational harmonic mode-locked laser and identified the effective modulation depth is contributed by the higher order harmonics from the RF amplifier.

Third, we have successfully demonstrated an asynchronous rational harmonic mode-locked fiber laser with the repetition rate up to 33 GHz. From the results of Chapter 3.3, the sidemode suppression ratio and SMSR is very well.

One important thing here is that the pulse repetition rate can go beyond

the RF amplifier bandwidth in this case.

Finally, we found a new mode-locked state and have designed a series of experiments to check the characteristics of this new mode-locked state. Under this new state, the SMSR can be greater than 55 dB, limited by the measurement equipment. The deviation frequency variation is very small and is related to pumping power proportionally. From all the experimental results, we conclude this new state is synchronous mode-locking with sidebands instead of asynchronous mode-locking.

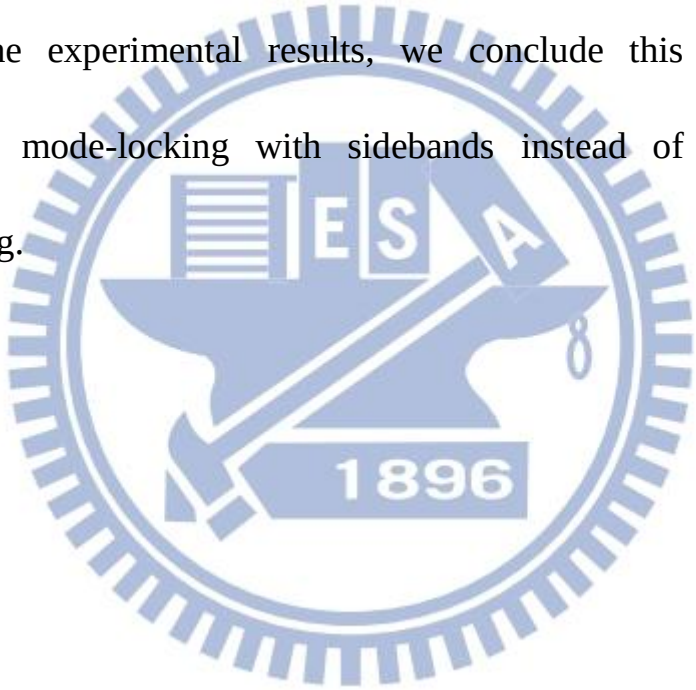

4.2 Future work

The thesis work has successfully demonstrated a 33 GHz asynchronous rational harmonic mode-locked Er-doped fiber soliton laser. However, the duration of stabilization is too short to measure the laser dynamics. This is because the intacavity optical power is somewhat reduced by our new optical delay line, which causes the laser operation to be not very stable. One obvious solution is to replace with high nonlinear fibers to enhance the nonlinear effects. The estimated effective modulation depth is also not very close to the experimental values. We will exercise a set of experiments to produce a map with varying modulation depths. Finally, the new state of synchronous harmonic mode-locked fiber laser provides us high SMSR and long-term stabilization mechanism by the deviation-frequency locking. However, we still do not exactly know the characteristics of the deviation frequency in this case. We also do not know why the new state can provide so excellent performance in the presence of gain dynamics. We shall explore more about these unknown for the new mode-locked state in the future.